U.S. DEPARTMENT OF ENERGY

PNNL-24904

Prepared for the U.S. Department of Energy
under Contract DE-AC05-76RL01830

Energy Savings Potential of Radiative Cooling Technologies

N Fernandez
W Wang
K Alvine
S Katipamula

November 2015

Pacific Northwest
NATIONAL LABORATORY

Proudly Operated by Battelle *Since 1965*

DISCLAIMER

United States Government. Neither the United States Government nor any agency thereof, nor Battelle Memorial Institute, nor any of their employees, makes **any warranty, express or implied, or assumes any legal liability or responsibility for the accuracy, completeness, or usefulness of any information, apparatus, product, or process disclosed, or represents that its use would not infringe privately owned rights**. Reference herein to any specific commercial product, process, or service by trade name, trademark, manufacturer, or otherwise does not necessarily constitute or imply its endorsement, recommendation, or favoring by the United States Government or any agency thereof, or Battelle Memorial Institute. The views and opinions of authors expressed herein do not necessarily state or reflect those of the United States Government or any agency thereof.

PACIFIC NORTHWEST NATIONAL LABORATORY
operated by
BATTELLE
for the
UNITED STATES DEPARTMENT OF ENERGY
under Contract DE-AC05-76RL01830

Printed in the United States of America

Available to DOE and DOE contractors from the
Office of Scientific and Technical Information,
P.O. Box 62, Oak Ridge, TN 37831-0062;
ph: (865) 576-8401, fax: (865) 576-5728
email: reports@adonis.osti.gov

Available to the public from the National Technical Information Service,
U.S. Department of Commerce, 5285 Port Royal Rd., Springfield, VA 22161
ph: (800) 553-6847, fax: (703) 605-6900
email: orders@ntis.fedworld.gov
online ordering: http://www.ntis.gov/ordering.htm


This document was printed on recycled paper.
(8/00)

PNNL-24904

Energy Savings Potential of Radiative Cooling Technologies

N Fernandez
W Wang
K Alvine
S Katipamula

November 2015

Prepared for
U.S. Department of Energy
under Contract DE-AC05-76RL01830

Pacific Northwest National Laboratory
Richland, Washington 99352

Executive Summary

Pacific Northwest National Laboratory (PNNL), with funding from the U.S. Department of Energy's (DOE's) Building Technologies Program (BTP), conducted this scoping study to estimate the potential cooling energy savings through the use of free radiative cooling in buildings, particularly photonic 'selective emittance' materials.

Selective emittance materials show high technical potential for radiative cooling applications by reflecting a very large fraction of incident solar radiation while increasing longwave radiative exchange with the relatively cool sky. Recent work by Stanford University has applied a photonic approach to tailor the optical properties of a coating material. The resulting photonic radiative cooler has demonstrated surface temperatures below ambient temperature when exposed to direct sunlight. This achievement represents a technological breakthrough, and may have the potential to transform the market for radiative cooling in buildings (which to-date has been a small niche market) through the novel provision of free cooling during the day as well as at night.

The advances in daytime radiative cooling are promising for building applications. However, it is difficult to translate the experimental results from research prototypes to meaningful energy savings in buildings. Many factors such as system configuration and controls, space cooling load profiles and the weather will affect the potential energy savings. It is also valuable to know the incremental benefits of daytime radiative cooling relative to conventional nocturnal radiative cooling. In such context, PNNL used building energy simulation to estimate the energy savings from daytime radiative cooling, specifically based on photonic materials.

Approach

PNNL conducted a literature review on applications of radiative cooling to provision free-cooling for buildings and settled on a conceptual approach that is anticipated to best enable the use of a photonic radiative cooling heat exchanger to offset space cooling demands. This approach involved a hydronic delivery system for cooling energy into the building, consisting of two loops; a rooftop heat exchanger loop, and a building cooling loop, both coupled to a cold water storage tank. The building cooling loop draws water from the tank, and performs any necessary final cooling via a chiller before distributing chilled water to radiant floor slabs in each thermal zone of the building. The same slabs can be utilized for heating as well, and are connected to a hydronic heating loop with a natural gas boiler.

This configuration was investigated in a medium office building because medium-sized office buildings are the most common size of office buildings and because space usage is often similar to some other commercial building types. The building model originated from the building energy codes program, which maintains a series of EnergyPlus models in compliance with different versions of commercial codes. This version is compliant with 2013 commercial building codes, because the proposed technology is suited almost exclusively for new construction. The building has three floors and a total floor area of 5000 m^2. Several reference systems were established to quantify the potential of energy savings from the photonic radiative cooling system. The reference systems include 1) a variable-air-volume (VAV) system that represents the prevailing technology used to condition medium-sized office buildings; 2) a hydronic radiant system that forms the basis to understand the marginal benefits of adding radiative cooling; and 3) a nighttime radiative cooling system using conventional materials that can be regarded as a lower-cost, competing alterative to the photonic radiative cooling system. The savings analysis was made for a five locations in four different climates, namely, Miami, FL (hot and humid climate); Las Vegas, NV and Los Angeles, CA (hot and dry climate); San Francisco, CA (marine climate); and Chicago, IL (cold climate).

EnergyPlus does not support the specification of rooftop radiative heat exchangers, so custom heat transfer modeling was applied to simulate the flows of heat between the heat exchanger, building, and sky, and the anticipated hydronic loop conditions were passed back into the EnergyPlus model. This custom modeling was performed in EnergyPlus's energy management system (EMS) framework, which allows the user to build equations that overwrite certain pre-determined points of intervention in the EnergyPlus model. For the nighttime radiative cooler, first-principle thermodynamic equations were used with some simplifying assumptions to model heat flows for conventional heat exchanger surfaces. PNNL partnered with researchers at Stanford who developed the photonic surfaces being investigated for radiative cooling. The researchers provided PNNL with detailed spectral characterizations of the thermodynamic properties of their material. Calculation of radiative heat transfer from photonic materials, however, required mathematical integration functions that are not supported by the EMS. To get around this problem, PNNL used a regression equation for radiative heat exchange based on an integration performed in MATLAB, developed by the Stanford researchers.

Results

Relative to the VAV system, the proposed photonic radiative cooling system saves 103 MWh electricity in Miami, 55 MWh in Las Vegas, 50 MWh in Los Angeles, 24 MWh in San Francisco and 43 MWh in Chicago, per year. The saved electricity represents 50%, 45%, 65%, 68%, and 55% of the VAV system cooling electricity, respectively in the above five cities. Relative to the high-end nighttime radiative cooling products available in the market, the photonic radiative cooler saves 10 MWh electricity in Miami, 13 MWh in Las Vegas, 8 MWh in Los Angeles, 3 MWh in San Francisco and 6 MWh in Chicago, per year, which represents 9%, 16%, 23%, 22%, and 14% of cooling electricity savings, respectively in the above five cities.

Market Assessment and Conclusions

Radiative cooling in buildings is best harnessed with hydronic distribution systems. Because achievable chilled water temperatures from radiative cooling are typically well above chilled water temperatures required for forced-air-based delivery systems, this necessitates the simultaneous specification of radiant zone cooling. Both radiative cooling and radiant zone cooling are investigated for market benefits and barriers.

There are a wide variety of mechanisms by which radiant cooling and its required set of technologies can produce benefits to building owners and occupants. These include energy savings (and associated energy cost savings), other cost savings from elimination of alternative heating, ventilation and air conditioning (HVAC) infrastructure and downsizing of equipment as well as improved comfort. Besides providing additional electric energy savings, a system that integrates the radiative cooling heat exchanger to a building cooling loop via a cold water storage tank may be a very favorable participant in demand response.

Several market barriers exist for which recommended mitigation strategies are provided. The barriers are that radiative cooling solutions are not well suited for existing buildings/retrofits, additional installation costs, complexity and the need for holistic design, as well as limitations imposed by climate, by certain building shapes, and by space available for new equipment.

A simple economic analysis shows that for upgrading the new construction design from a VAV systems for HVAC delivery to photonic radiative cooling with radiant zone cooling, the maximum incremental cost for a 5-year simple payback ranges from $8.25 to $11.50 per square meter of total building floor area, based on climate. For an upgrade from nighttime radiative cooling using conventional materials to photonic radiative cooling, the maximum incremental cost for a 5-year simple payback is $2.50 to $6.25 per square meter of rooftop heat exchanger area.

Acknowledgments

The authors would like to acknowledge the Building Technologies Office of the U.S. Department of Energy for funding the study. Many thanks go to Drs. Aaswath Raman, Shanhui Fan, and Eli Adam Goldstein, the researchers at Stanford University who developed the novel photonic radiative cooler product, for sharing their MATLAB program used to calculate the net radiative heat transfer with the sky and for discussing the project several times. Dr. Michael Witte from Gard Analytics helped on the EnergyPlus modeling.

Table of Contents

List of Figures

List of Tables

Symbols and Abbreviations

A	area
AHU	air-handling unit
amb	ambient
ASHRAE	American society for Heating, Refrigeration and Air-Conditioning Engineers
AUST	area-weighted average temperature
BTP	Buildings Technology Program
cond	conduction
conv	convection
COP	coefficient of performance
c_p	specific heat capacity
DOAS	dedicated outdoor air system
DOE	Department of Energy
dp	dewpoint
dT	simulation timestep
DV	displacement ventilation
$Elec$	annual electricity consumption (kWh)
EMS	energy management system
f	air film
F_{p-i}	angle factor between a person and a surface
FCU	fan coil units
g	acceleration caused by gravity
Gr	Grashof Number
h_c	convection coefficient
HVAC	heating, ventilation and air conditioning
I	irradiation
IC	maximum acceptable incremental cost
IR	infrared
ISO	independent system operator
k	thermal conductivity
K_0	a measure of sky cover
LWX	longwave
L_n	characteristic length for natural convection (area to perimeter ratio)
L_{eff}	effective length
$\dot{m}$	mass flow rate

mr	mean radiant
N	opaque sky cover fraction
NG	annual natural gas consumption (Therm)
O&M	operations and maintenance
oper	operative
ORNL	Oak Ridge National Laboratory
p_d	partial pressure of water vapor in air
PCM	phase change material
PE	polyethylene
PNNL	Pacific Northwest National Laboratory
PPO	polymer resin
Pr	Prandtl Number
PV	photovoltaic
PV/T	photovoltaic/thermal
Q	heat transferred per unit time
q	heat flux (heat transferred per unit area and per unit time)
r	price for electricity or natural gas ($)
rad	radiation
Ra	Raleigh Number
RC	radiative cooling
Re	Reynolds Number
R_f	surface roughness factor
SE	selective emittance
t	current timestep
Δt	elapsed time since previous timestep
T	temperature
TABS	thermally active building systems
V	volume of water per segment of heat exchanger
VAV	variable air volume
w	wind speed
X	length
X	current segment of heat exchanger
Δx	thickness
Y	payback period in years
α	absorptivity
ε	emissivity
λ	wavelength (electromagnetic spectrum)

η	weighting factor for natural convection
σ	Stefan-Boltzmann Constant (5.67×10^{-8})
ρ_w	density of water
τ	transmissivity
μ	fluid viscosity

1. Introduction

Radiative cooling refers to the physical process by which a body loses heat to another body of lower temperature via long-wave radiation. In the case of buildings, radiative cooling results from the thermal radiation exchange between building surfaces on the Earth and the colder atmospheric layers in the sky. Utilizing radiative cooling to achieve energy savings in commercial buildings remains a largely untapped potential. Applying the source of cooling outside of the thermal envelope to the thermal load inside the building requires additional design considerations, technological components, and coordination of systems. Because of these complexities and other market barriers (including limited technical potential) of conventional designs for utilizing radiative cooling, it has only been involved in a few fringe applications to offset demands for mechanical space cooling in buildings. However, new advances in composite materials with favorable radiative cooling properties have emerged recently that have revived interest in radiative cooling as a potentially viable economic solution for reducing energy consumption for space cooling. Specifically, "selective emittance" or "photonic" radiative cooling devices, which have been characterized by high exchange of longwave radiation with the sky and very low absorption of solar radiation has garnered interest as a result of claims of the device's potential to maintain a surface temperature below the ambient air even when exposed to intense, direct sunlight.

This report attempts to assess through building energy modeling the potential of a photonic approach to selective emittance materials, applied to the technological solution of provision of free cooling energy to offset mechanical cooling in commercial buildings. This quantitative assessment of energy savings is combined with a qualitative market assessment of radiative cooling to facilitate an understanding of the viability of this technology and requirements for a path to market adoption. This report frames radiative cooling as part of a technological solution set that builds upon other advanced building energy technologies, especially radiant space cooling with dedicated outdoor air systems for ventilation. These prerequisite technologies are discussed in depth in this report as they relate to a built-up system that facilitates the use of radiative cooling. The benefits and barriers of those systems are important to understand in that context as well.

Section 2 of this report provides a literature review of radiative cooling in buildings as well as radiant cooling technologies for space cooling. Section 3 describes the technical approach used to determine potential energy savings from novel radiative cooling technologies. Section 4 describes the modeling framework and equations used to simulate radiative cooling heat exchangers and how this simulation is integrated with conventional building energy modeling software. Section 5 describes the results of the modeling work, discussing potential energy savings in different climates, a simple economic analysis, as well as a more in depth discussion of the performance of the rooftop radiator. Section 6 provides a market analysis of radiative cooling and discussion of benefits and potential market barriers. Conclusions are provided in Section 7.

2. Radiative Cooling and Radiant Cooling Literature Review

A review of the existing theoretical literature as well as documented installations of radiative cooling in buildings is provided in Section 2.1. A review of radiant cooling technologies is also provided in Section 2.2

2.1 Radiative Cooling

For buildings in most climates, some very limited radiative cooling takes place naturally at night throughout the cooling season. This can occur whenever the *effective sky temperature* is colder than the roof surface of the building, creating a net radiative outflow of heat to the surroundings. The term *effective sky temperature* is often used to simplify the complex phenomenon of thermal radiation between building surfaces with the atmosphere. Thermal radiation is emitted by all ground surfaces, including building rooftops. Some of that radiation is reflected back to the ground from the atmosphere or absorbed by the atmospheres (greenhouse effect), and the atmosphere emits some of its own thermal radiation to the ground as well. The degree to which radiation is reflected back to the ground and emitted by the atmosphere changes in complex ways in response to changes in temperatures and humidity levels in different layers of the atmosphere as well as the presence, thickness, and altitude of different cloud layers. To simplify the problem mathematically, the sky is typically considered to be a single entity with a uniform or average radiative temperature that can be applied to the Stefan-Boltzmann equation (Eq. 1) to calculate the net exchange of radiative heat ($Q_{radiative,net}$) between the building and the sky, where in Eq. 1, σ is the Stefan-Boltzmann constant, ε is the surface spectral and directional average blackbody emissivity of the roof, A_{roof} is the roof area in m^2, and T_{roof} is the exterior surface temperature of the roof in °C.

$$Q_{radiative,net} = \sigma \varepsilon A_{roof} \left((T_{roof} + 273.15)^4 - (T_{sky} + 273.15)^4 \right) \quad (1)$$

Radiative cooling takes place when T_{sky} is lower than T_{roof} in Eq. 1. Many researchers have developed clear-sky correlations to relate the effective sky temperature during clear conditions to ground measurements of ambient temperature and humidity. Many of these clear sky correlations are summarized in (Eicker and Dalibard 2011). Clouds, however, also strongly affect the effective sky temperature, and some researchers have attempted to include sky cover (cloudiness) as part of correlations for calculating sky temperature. Aubinet (1994), for example, proposed the following correlation for T_{sky} that includes a measure of sky cover, K_0 and uses the water vapor partial pressure p_d as a measure of humidity.

$$T_{sky} = 94 + 12.6 \cdot \ln(p_d) - 13K_0 + 0.341 T_{amb}. \quad (2)$$

The Department of Energy's building comprehensive building energy modeling software, EnergyPlus (US DOE 2013) uses sky emissivity and ambient air temperature ((T_{amb}, °C) to calculate the sky temperature via Eq. 3. The sky emissivity is determined via a correlation (Eq. 4) from Clark and Allen (1978) and uses the dewpoint temperature (T_{dp}, °C) and the opaque sky cover, N (0 to 1) to predict sky emissivity, ε_{sky}.

$$T_{sky} = \varepsilon_{sky}^{\frac{1}{4}} (T_{amb} + 273) \quad (3)$$

$$\varepsilon_{sky} = \left[0.787 + 0.764 \cdot \ln\left(\frac{T_{dp} + 273}{273} \right) \right] \cdot \left(1 + 0.224N - 0.0035N^2 + 0.00028N^3 \right) \quad (4)$$

Using these correlations, the effective sky temperature can be as much as 30°C cooler than ambient temperature during clear sky conditions with low humidity, but may be close to the ambient temperature during humid, cloudy conditions. It is this difference between the ambient and sky temperatures that presents an opportunity for free radiative cooling.

The primary reason why radiative cooling of buildings is typically very limited lies in the necessity to insulate the underside of the roof (or the top side of the attic) to protect the building from direct solar radiation on hot summer days and from the loss of heat from the roof during the heating season. This insulation also severely limits potentially beneficial heat rejection from the building to the cool night sky during the cooling season (especially at night). Radiative cooling strategies are all variations on designs that seek to enable better heat rejection from the roof when it is appropriate, and to utilize the resultant cooling energy to reduce the need for mechanical cooling. These strategies fall into the following categories based on their design:

- Utilizing **movable insulation** to selectively remove the barrier to significant free cooling
- Active or **"hybrid" systems** that use either air flow or hydronic systems to deliver radiative cooling to spaces
- **Selective emittance materials or coatings.**

2.1.1 Moveable Insulation

The design principle behind movable insulation is that passive cooling energy can be transmitted to the building spaces by designing buildings with the insulating layer as the outer surface of the roof and mechanically removing the insulation when the building can be cooled via radiative cooling. Raeissi and Taheri (2000) modeled a system called *Skytherm* and validated this model against field data from a house equipped with this system in Shiraz, Iran. In the *Skytherm* system, water 'ponds' were contained in clear plastic bags that sat on top of a metal deck or concrete surface of the roof. This underlying roof surface was painted to increase its emissivity and make it a better radiator. 2-inch thick polyurethane insulation boards with aluminum skins were used as movable insulation and placed on top of the pond bags. During a summer day in June when data was collected on the actual house, the maximum cooling energy flux delivered to the interior of the house from the bottom of the roof was between 17 and 18 W/m^2 around sunrise with a minimum between 7 and 8 W/m^2 in the late evening. Cooling was maximized with a thin metal underlying roof surface, and was lower for the thick concrete deck. Total cooling loads were reduced by 52% with this system. It should be noted, however, that the test building was only evaporatively cooled (no vapor-compression systems), and was thus unlikely to be able to maintain the kind of temperature control available in most modern buildings. The cooling flux provided to the building may have been high because internal temperatures were above the comfort conditions specified by American Society for Heating, Refrigeration and Air-Conditioning Engineers (ASHRAE 2013).

The *Skytherm* system should be considered proof of concept at best because presumably, for this system to be feasible, the movable insulation would have to be constrained so that it would not be blown away during strong windy days. Also, the system is not likely to be used frequently unless the insulation could be moved automatically.

Cavelius et al. (2007) pointed out the advantages and disadvantages with movable insulation systems. One advantage is that the system can work in reverse in the winter by collecting solar heat during the day, then insulating at night. The major disadvantages are that the system is expected to be expensive if the insulation is movable through automatic means, and that this system becomes less advantageous to multi-

story buildings because only the top floor will benefit from the passive cooling provided from the ceiling on the underside of the roof. If the insulation is not moveable automatically via a control system, it is unlikely to be utilized frequently or properly to maximize night cooling.

2.1.2 Hybrid Systems

Hybrid systems attempt to avoid the problems of moveable insulation by using active transport of either air or water along with automatic control systems to deliver cooling to the building spaces.

There are a relatively limited set of concepts for hybrid systems using air as the heat-transfer medium. Parker (2005) presented a theoretical evaluation of a concept called *NightCool*. In this concept, the air in the attic space is used as a potential source of return air for the air-conditioner's indoor unit. A special white-painted metal roof on metal battens (rather than typical roof decking) is used to maximize longwave radiative cooling and to maximize heat transfer between the roof and the attic space, while minimizing rooftop absorption of solar radiation during the day. The system requires a special damper that either selects air from the attic or from the main living area to use as return air. This is similar to the use of an outdoor/return air damper on typical commercial air handlers. The concept also includes the use of a small, portable de-humidifier in the attic to guard against mold and condensation when the attic humidity becomes too high.

Parker (2005) reported that during the month of July, the average daily cooling available from this system ranged from 63 to 110 Wh/m^2 of roof surface, depending on the U.S. climate location. The amount of cooling was also sensitive to many other factors, especially the return air temperature that was brought into the attic space for cooling. This *NightCool* concept may only be feasible during the hot summer months in many locations, for example, when the indoor thermostat is kept relatively high (23.9°C or above). Thus, the *NightCool* concept (and indeed all radiative passive cooling strategies) cannot provide fixed capacities of cooling, but instead act as negative feedback mechanisms on internal zone temperature - the warmer it gets inside the building, the more cooling is available. The cooling available is also very sensitive to the flow rate of return air through the attic, with a larger flow rate producing more cooling, asymptotically approaching a maximum cooling limit that is driven by the rate of heat transfer from the metal roof (Parker 2005). The total cooling savings predicted for a house in Tampa, Florida during the summer months of June through September was 46%. The methodology used to calculate this fraction is very questionable, however, because it is simply dividing estimated daily cooling provided by the *NightCool* system by the estimated total daily cooling load. This estimate seems high in a climate like Tampa, given that the majority of the cooling loads occur during the day, and this can only operate during limited nighttime hours. Including the fan and dehumidifier energy consumption as the electric input required for this system, Parker calculated the coefficient-of-performance (COP) over these 4 months to be 10.9 for Tampa, FL and as high as 26.0 for Baltimore, MD.

The main limitation of the *NightCool* concept is that it only really applies to new single-family residential homes, and that this concept cannot be retrofitted into an existing home (because it requires a special roof design). It would be interesting to see how this concept performs in comparison with adding an outdoor air economizer to the residential air-conditioning unit in climates with relatively cool summer nights.

Another hybrid system using air as the heat transfer medium was proposed by Mihalakakou et al. (1998). They simulated the performance of a metallic radiator where air is cooled through forced convection (fan-power) under the metallic surface of the radiator, and is then directed into the building. Depending on the wind speed (from 1 to 2.5 m/s) and cloudiness, they calculated that the radiator could provide 30 to 55 Wh/m^2 of cooling on a typical July day in Legnano, Italy. While using forced air within the radiator

eliminates the cost of a hydronic loop, air-side pressure drops are likely to be high, forcing higher fan power consumption.

Hybrid radiative systems using hydronic systems to deliver and store radiatively-cooled water are more common in the literature and are more versatile in application. Meir et al. (2002) presented a field study of a hybrid system in which water flows through twin-walled PPO (polymer resin) radiators installed on the roof of a building. In the experimental setup, the water was circulated through the radiator, then stored in a reservoir, before being pumped back up to the radiator. The purpose of the study was to demonstrate the cooling power available from such a system. The radiator is similar in design to a simple solar hot water heater's collector, and indeed, radiators like this could be used for both space heating and cooling. Meir found that on completely cloudy nights, when the radiator temperature was equal to the outdoor ambient temperature (T_{amb}), there was no cooling power. This increased to 100 W/m^2 when the radiator temperature was 10°C warmer than T_{amb}. When skies were clear, cooling heat flux was around 60 W/m^2 when the radiator temperature was equal to T_{amb} and increased to 160 W/m^2 when the radiator temperature was 10°C warmer than $T_{amb.}$ An interpretation of these findings is that the presence of clear conditions appears to add a cooling heat flux of 60 W/m^2 to the radiator and that convection will add approximately 10 W/m^2 for every 1°C warmer the radiator is, compared to $T_{amb.}$ An extrapolation of these findings then suggests that such a radiator is likely capable of cooling water to a minimum of 6°C below T_{amb}, given clear conditions.

Collins and Parker (1998) reviewed the performance of three types of hybrid radiative and evaporative cooling systems manufactured by Roof Science Corporation under the trade name *WhiteCap*. The three systems are referred to as *WhiteCapR*, *WhiteCapF*, and *WhiteCapT*.

WhiteCapR is a design that involves maintaining a 76-mm layer of water on top of the roof at all times. On top of this layer, interlocking polystyrene panels float, and the tops of these panels are sprayed with water that is evaporatively and radiatively cooled, then drains to the water layer below the panels. A separate building cooling loop pumps the cooled water to radiant cooling panels within the building (see Figure 1).

In *WhiteCapT* and *WhiteCapF*, the roof is slightly sloped. A thin layer of water is pumped to the roof, coating the surface, and draining into a building loop. In the *WhiteCapT* configuration (Figure 2), the water is pumped to the roof at night and drains into a storage tank. During the day, cool water stored in the tank is pumped through interior fan-coil units to provide cooling on-demand. In the *WhiteCapF* configuration (Figure 3), the water draining from the roof is pumped into slab foors at night before retuning to the rooftop, storing the cooling in the building's thermal mass.

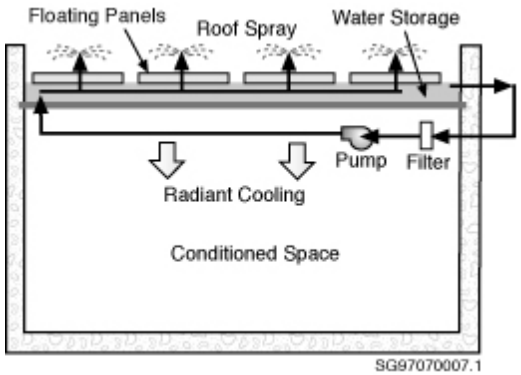

Figure 1: WhiteCapR schematic from Collins and Parker (1998).

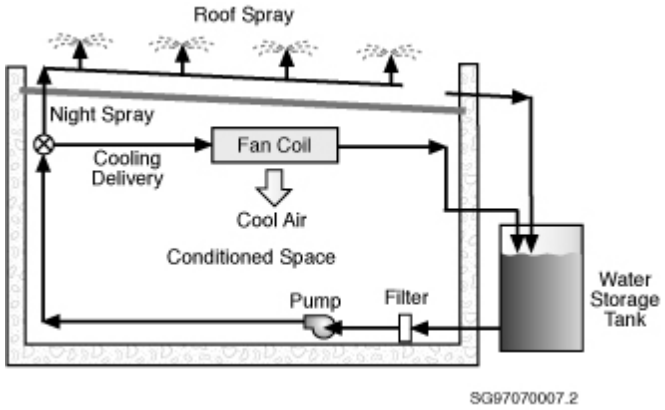

Figure 2: WhiteCapT schematic from Collins and Parker (1998).

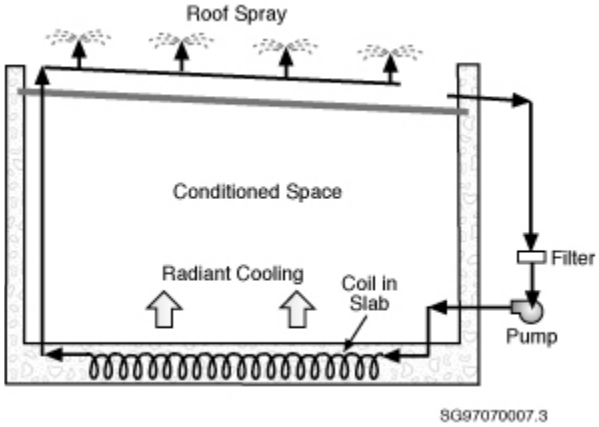

Figure 3: WhiteCapF schematic from Collins and Parker (1998).

WhiteCap installations in various sites (mostly in California) have provided between 30% and 60% of the buildings' annual cooling loads. In climates with cool (below 18.3°C at night during summer) and dry conditions, the typical WhiteCap capacities are 3.5 MJ/m^2 of roof area.

Collins and Parker (1998) evaluated the installation of a *WhiteCapT* installation in Nogales, Arizona and documented an average COP of 149 from April to August 1997.

The three *WhiteCap* systems rely on a combination of evaporative and radiative cooling, rather than other technologies that may provide cooling purely through radiative means. The disadvantage of adding evaporative cooling is that it consumes water (trading increased water consumption for energy savings). Although this is definitely a trade-off, the cooling energy available from the latent heat of water at room temperature is 2400 kJ/kg, meaning that 3.78 liters (1 gallon) of water can provide 8,700 kJ (2.42 kWh) of cooling. Assuming that this cooling displaces conventional cooling from packaged units with a COP of 3, 1 gallon of water costing 1.5 cents per gallon may provide cooling that can displace electricity costing 8.7 cents (at 10.8 cents per kWh). It is also worth noting that most large commercial buildings throughout the country use cooling towers for condenser heat rejection that already utilize evaporation of water to provide a cooling benefit.

The Roof Science Corporation is not the only company commercializing systems similar to *WhiteCap*. Cavelius et al. (2007) summarized the *Batiso* system by German manufacturer Zent-Frenger. This system is nearly identical to the *WhiteCapT* configuration. Oak Ridge National Laboratory (ORNL 2014) created a system called "*NightSky*", manufactured by Integrated Comfort, Inc. using a similar water-sprayed roof

concept, draining into a storage tank. This system was installed at a site in Vacaville, CA. The tank water flows through a radiant cooling slab to pre-cool the building, before the water is cooled further by a chiller and sent to chilled water fan-coil units. The roof cooling part of the system was documented to provide 2/3 of the total cooling to the building at a COP of 58.7. Rooftop spray-cooling systems are popular in commercialized technologies because of the low costs involved. Compared to covering a large fraction of the roof with radiators and using tubing to flow water, the rooftop itself can be used as the radiator, and the water can flow across the roof with no flow resistance to the pump. The additional cost of the *NightSky* system in Vacaville, CA was $\$14.53/m^2$ of building floor area, and the cost of the *WhiteCapT* system in Nogales, AZ was $\$36.75/m^2$ (both cost figures are for late-1990s U.S. dollars).

Eicker and Dalibard (2011) presented the results of a field study of a novel application for radiative cooling in Madrid Spain. In this configuration, photovoltaic (PV) panels are used as radiators, with water pipes embedded on the underside of the PV. The water is pumped through a circuit that cools a phase-change material (PCM) with a 22°C melting point at night (latent heat storage) that is embedded in the thermal mass of the building. The constant temperature heating/cooling process provides a distinct advantage over water storage because radiative cooling can occur without reducing the driving temperature difference between the radiator and the sky (as would normally occur with sensible cooling). Eicker and Dalibard (2011) reported annual cooling of 51 kWh/m^2-year, with cooling power at night ranging between 40 and 65 W/m^2. The COP of the system ranged from 17 to 30.

Zhang and Niu (2012) have also proposed using phase-change materials for night radiative cooling applications, but in the form of micro-encapsulated beads within slurry. They proposed hexadecane (melting temperature of 18°C) for the PCM material and simulated its performance using a flat plate radiator in five locations in China. The melting temperature for this medium is rather low, however, and has poor performance in the summer months except in very cool climates, where the radiator's surface temperature can more frequently drop below 18°C during the cooling season.

2.1.3 Selective Emittance Materials or Coatings

Selective emittance (SE) materials have high technical potential for radiative cooling applications (Catalanotti 1975). Such a material coating could allow for greater technical potential by tailoring the thermal heat losses as well as incident radiation. In the context of radiative cooling, heat losses occur in the infrared (IR), where the 300K blackbody radiation is peaked at approximately 10 microns. The blackbody radiation peak shifts to shorter wavelengths with higher temperatures, but is still in this approximate range for most buildings applications. As noted previously, the theoretical maximum for radiative cooling (RC) is given as $120W/m^2$ (Granqvist 2003) or $150W/m^2$ (Rephaeliet al. 2013), according to different studies. This offers a cooling temperature drop up to 34°C with an assumed $1W/m^2K$ non-radiative heat influx. (Granqvist 2003) Selective emittance materials potentially offer the additional option of daytime RC, in addition to nighttime RC.

Daytime RC is highly sought after because this would better offset peak cooling loads, as well as effectively double the average daily cooling. However, realizing such daytime cooling technology is severely complicated by both solar irradiance heating of structures between 0.25 and 3 microns with approximately 1300 W/m^2 (Granqvist 2003) and also by atmospheric absorption as already mentioned. Solar irradiance will easily swamp any RC cooling effect without an effective solar irradiation heat shield in place during most of the day. Atmospheric absorption is problematic in that building heat is coupled into the surrounding air and cannot be readily dissipated. This is further complicated by sky conditions. There is however, a range in the IR between 8 to 13 microns where atmospheric absorption is negligible and the buildings thermal radiation can effectively be transported to space without appreciable heating of the surrounding air. Thus, for optimal cooling, the spectral emittance of a building envelope coating would then be (Granqvist 2003):

$R(\lambda) = 1$ for $0.3\ \mu m < \lambda < 3\ \mu m$ (Daytime Radiation Shield)

$R(\lambda) = 0$ for $8\ \mu m < \lambda < 13\ \mu m$ (For Thermal Emission[1])

For nighttime only radiative cooling, the requirements are relaxed because the radiation shield requirements are not needed. In fact, for a cool, dry climate with clear skies, greater nighttime cooling may be realized if the thermal emission range is expanded somewhat to better match the blackbody radiation curve when water absorption is minimized. More importantly, the 8- to 13-micron window however, is not affected by humidity or overcast skies, but is affected by wind and parasitic heat losses (Granqvist 2003, Raman et al. 2014, Rephaeli et al. 2013). If the thermal emission constraint is broadened, then water absorption and sky condition (overcast vs clear) become a significant factor, dropping the cooling rate by a factor of two or more (Niklasson and Nilsson 1995, Nilsson et al. 1992). Thus, there may be regional variations where relaxations of these constraints are effective.

Several approaches to fabricate materials that meet the strict selective emittance requirements stated above have been investigated since at least the mid 1980s (Niklasson and Nilsson 1995, Nilsson et al. 1992, Berdahl 1984, Eriksson and Granqvist 1986, Tazawa et al. 2006). Unfortunately, this dual set of requirements is highly demanding and much of the research into advanced materials is still in the very early stages (Raman et al. 2014, Rephaeli et al. 2013, Zhu et al. 2013, Zhu et al. 2014) Metals for example, can provide high reflectivity for solar irradiance, but they also have poor emittance in the IR and are not suitable.

It should be noted however, that partial forms of the radiation shield component are already in widespread use in certain regions as the so-called "cool-roofing" products (Al-Obaidi et al. 2014). However, these products do not meet the strict reflectivity requirements above to block all solar irradiance, nor do they necessarily meet the thermal emittance window requirements. Additionally, these types of radiation shields are most efficient when white in color or only very lightly pigmented, which is not considered attractive for residential roofing application. This issue is sometimes referred to as "white blight", which can cause visible discomfort and glare and thereby cannot be used near flight paths (Al-Obaidi et al. 2014). Such color considerations and or fluorescence cooling (Epstein et al. 1995) need to be taken into account to further research into selective emittance coatings. One such approach using advanced materials that has been studied theoretically to date is to use advanced coatings utilizing the resonant properties of nanostructures to preserve the color (Zhu et al. 2013).

Much of the initial work on materials for spectrally-selective coatings focused on pigments such as ZnS, and ZnO that showed nighttime radiative cooling of up to 52 W/m^2 (Niklasson and Nilsson 1995, Nilsson et al. 1992). These have the advantage of being relatively easy to fabricate and deposit. Unfortunately, the reflectivity in the solar irradiance part of the spectrum was only approximately 80-85% or R=0.8 to 0.85. This meant that daytime radiative cooling was not possible, with the exception of early morning or late evening when the solar irradiance was low. Additionally, ZnS is not stable under prolonged solar irradiance (Mastai et al. 2001). Other pigments, including TiO_2 are possible candidates, but still do not meet the high reflectivity needed for daytime cooling (Mastai et al. 2001, Granqvist 2003).

Other approaches for nighttime radiative cooling selective emittance films included sputtered multilayer dielectric films on Al backing (infrared reflective) such as MgO, MgF, LiF, SiO_2, oxynitride, and others (Eriksson and Granqvist 1986, Granqvist 2003, Berdahl 1984, Tazawa et al. 2006). For example, spectral selectivity can be achieved by 1-micron thick silicon oxide and oxynitride films backed by Al (Eriksson and Granqvist 1986, Granqvist 2003, Granqvist and Hjortsberg 1981). Drawbacks are that these films

[1] Note that thermal absorptivity is the inverse of reflectivity for an opaque surface and that spectral emissivity tends to be nearly identical to spectral absorptivity for real surfaces. Thus, a surface with a spectral reflectivity around 0 at certain wavelengths would thus be expected to emit radiation.

must be very thick (1 micron or more), multiple materials are needed to cover the full window from 8 to 13 microns, and there is overlap outside of the atmospheric window. Other technology solutions include the use of thick gas slabs of NH_3, C_2H_4, C_2H_4O, or mixtures on Al backings. These have molecular vibrations that match well with the atmospheric window (Granqvist 2003). A drawback is that these must be about 10-cm thick, which is difficult to incorporate into building infrastructure. Still other options include Tedlar, a polyvinyl-fluoride plastic produced by Du Pont (Catalanotti 1975). Again, problems arise from significant absorptions outside of the 8- to13-micron band.

Because of the inability of standard materials to meet the strict requirements of the SE daytime radiative cooling stated above (Rephaeli et al. 2013, Gentle and Smith 2010), there has been recent research into advanced materials with tailored optical properties to fill the need. Primarily this has been through the use of nanomaterials or nanostructured and microstructured thin films (Raman et al. 2014, Rephaeli et al. 2013, Zhu et al. 2013, and Zhu et al. 2014). As stated above, much of this work is at the very early research stages and in some cases is not yet shown experimentally even at the laboratory scale.

One example of nanostructured coatings developed for radiative cooling is the recent work done by a research team at Stanford University (Raman et al. 2014, Rephaeli et al. 2013, Zhu et al. 2013, Zhu et al. 2014). These advanced coatings are based on coatings made up of one- and/or two-dimensional photonic structures. The incorporation of the micro or nano photonic layers allows the tailoring of the optical properties of the coating in ways not possible with bulk materials (Alvine et al. 2013, Rephaeli et al. 2013). In 2013, they published a study describing a theoretical SE claiming greater than 100 W/m^2 predicted daytime radiative cooling. This was based on a highly complex design that incorporated in excess of 30 deposited layers, including three sets of band-pass filters (one-dimensional photonic structures – periodic bilayers) and a two-dimensional photonic mesh-like structure. Another similar paper shows modeling results from visibly transparent two-dimensional photonic structures for solar cell radiative cooling (Zhu et al. 2014), and another shows that adaptions of these structures may be used for color preservation as mentioned above (Zhu et al. 2013). While the potential energy savings are impressive, it should be noted that 30 layers likely surpasses what is possible even in specialized window coatings currently available today and would likely be excessively expensive (e.g., V-Kool, Stellar Energy Solutions has seven layers, Comfort-Gard® Plus high performance glass has 15 or 16 layers). Secondly, no current technology exists in industry to fabricate the two-dimensional photonic structure in a low-cost fashion over large areas. The authors suggest roll-to-roll nanoimprint lithography (R2R NIL) as a possible route to this; however, R2R NIL has only just come into the market as a commercial tool in 2013 and this is likely not a near term solution. Alternate fabrication techniques, including template- or solution-based methodology with significantly fewer layers (<10), must be examined for this to be cost effective.

A more recent paper by Raman et al. (2014) describes experimental results from a much simpler seven-layer system that dispenses with the complex two-dimensional photonic structure; demonstrating an impressive 40 W/m^2 daytime radiative cooling. This system is not expected to perform as well as the more complex coating that includes the two-dimensional structure, but it does have the advantage of having significantly fewer layers and avoids the difficult to scale two-dimensional photonic structure. Also, seven layers more likely matches current glazing coating lines that exist today, although it would likely still be significantly more expensive than current roofing materials. Because the performance is down by more than a factor of two compared to the system with the two-dimensional photonic mesh-structure, additional research into cost-effective scalable methodology of making two-dimensional structures should prove fruitful.

Another possible technique to advanced radiative cooling materials is the use of nanoparticles (Gentle and Smith 2010). In a similar fashion to the photonic nanostructures, nanoparticles have vastly different optical properties than their corresponding bulk counterparts because of their size. The main advantage of nanoparticles (and pigments) over nanostructured coatings is that nanoparticles are typically better suited to wet deposition and in some cases can potentially be worked into paints or polymer melts (Gentle and

Smith 2010), The disadvantage is that the nanomaterial could be expensive, more difficult to control size and crystallinity, difficult to mass-produce, and less optical control is typically available because of the more random and/or polydisperse nature. Gentle and Smith (2010) have recently published theoretical and experimental results investigating radiative cooling with SiO_2 and c-SiC nanoparticles. The absorptive properties of the nanoparticle are well matched to the atmospheric 8- to 13- micron window. These would be incorporated into an inexpensive polyethylene (PE) film. The resultant cooling rates for these films was estimated to be 21 W/m^2 to 37 W/m^2. Similar investigations have also been performed with TiO_2 nanoparticles in PE films showing a modest 3°C temperature drop (Mastai et al. 2001). Potential issues arise from scattering outside of the atmospheric window as a result of the nanoparticle clustering and additional resonances. The full scattering over the solar irradiance was not reported, and it was not clear that these films by themselves would be useful for daytime radiative cooling.

While there are potential solutions currently to cost-effective nighttime radiative cooling, there are significant challenges to daytime radiative cooling, as shown above. The first is the severe restrictions on SE properties of the coating are not effectively met by traditional materials or multilayer coatings. To solve this issue requires the use of early advanced materials with nanostructures and/or microstructures or nanoparticle films. Because these are early in research and development, there are significant manufacturing and scale-up challenges despite the high technical potential (Rephaeli et al. 2013). Pathways to scalable and eventually cost-effective manufacturing at scale must be identified for these novel coatings.

It is worth noting that solar cell cooling is a synergistic research issue that aligns well with building radiative cooling. While there are significant differences, most notably the absence of the radiation shield requirement, the thermal emittance window requirements remain the same. Two-dimensional photonic structures have also been proposed for solar cell cooling (Zhu et al. 2014). This application and likely waste heat recovery may have a synergistic or catalytic effect on research in building radiative cooling. Other potential applications include water collection in arid climates (Granqvist 2003).

It is worth pointing out that dynamic material solutions should also be considered in the SE technology arena. Static radiative cooling coatings only have regional appeal and energy savings, and considerable additional savings and regional market appeal could be achieved if the radiative cooling could be made to be dynamic and operate only during cooling dominated months.

2.2 Radiant Cooling

A radiant cooling system refers to any system with a temperature-controlled surface that removes sensible thermal loads from a conditioned space mainly through thermal radiation (ASHRAE 2012). According to the heat transfer medium used to cool down the radiant surfaces, there are hydronic and non-hydronic radiant cooling systems. Because of its wide use, hydronic radiant cooling is elaborated in this section regarding its system types, controls, and advantages while non-hydronic radiant cooling such as thermoelectric cooling (Shen et al. 2013) is not discussed further.

2.2.1 Hydronic Radiant Cooling System Types

Babiak et al. (2009) identified the following three hydronic radiant systems: radiant cooling panels, embedded surface systems, and thermally active building systems. These three systems are briefly discussed below.

Radiant cooling panels are panels with integrated water pipes and they are fixed to building construction by hangers. Technically, both ceilings and walls can be used to attach radiant panels. In practice, however, most radiant cooling panels are suspended from ceilings. The radiant panels are usually designed as small modular units set into a metal frame substructure. To satisfy acoustical requirements, these panels can be perforated to make the ceiling sound absorbent when acoustic material is installed on the back of the panels. If the space cooling does not need fully covered radiant panels, conventional

acoustic panels can be used together with radiant panels to meet ceiling acoustic requirements (Weitzmann et al. 2008). ASHRAE (2012) presented three types of metal ceiling panels on the market for radiant cooling: the first type has modular aluminum panels (300 by 600 mm) attached to 15-mm galvanized water pipes; the second type features copper coils laid on a metal panel; and the third type features a metal panel with a copper tube mechanically fastened into a channel on the panel's back.

Embedded surface systems have water pipes embedded in the surface of building construction (floor, wall, and ceiling) and the surface layer with embedded water pipes is insulated from the building's structure. Five different types of embedded surface systems were described in ISO Standard 11855 (ISO 2012). These system types may have subtle differences with respect to the placement of water pipes (e.g., in the cement screed vs. in the insulation layer), the building construction type (e.g., concrete vs. wood), and the configuration of water pipes (e.g., regular water pipes to be installed on-site vs. preassembled capillary pipes).

Thermally active building systems (TABs) have water pipes thermally coupled to building structure (e.g., slabs and walls). The thermal coupling can be achieved by embedding water pipes in the massive concrete floor or by embedding capillary pipes in the plaster or gypsum board layer adjacent to the building structure (Figure 4). Depending on the desired heat transfer paths, thermal insulation may be added to on the top of the building structure. For example, without the thermal insulation (left side in Figure 4), the radiant floor can be used to cool the spaces both above and below the floor; however, with the thermal insulation layer added (right side in Figure 4), the radiant floor is used to cool only the space below. Feng et al. (2013) surveyed of radiant system experts about the current design practices of TABs. They found that:

- The depth of water tubes in the concrete slab depends on construction technique, code requirement and thermal inertia needs. Conventional practice is to place the tubes between 35 and 51 mm from the surface, but deep placement may be required in certain spaces such as retail stores to prevent water pipes being punctured by big bolts typically used for shelf anchorage (Doebber et al. 2010).
- Typical water tube diameters are 13 mm, 16 mm, and 19 mm.
- The spacing between tubes typically ranges from 150 to 300 mm on center. Closer spacing leads to a more uniform surface temperature and increased cooling output, but it also implies higher initial costs.

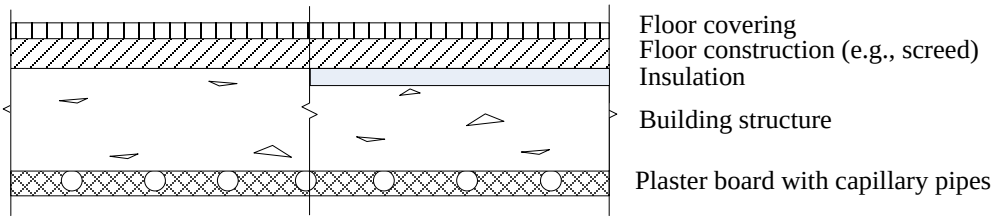

Figure 4: Section diagram of a thermally active building system with capillary pipes embedded in the plaster or gypsum layer

2.2. 2 Heat Transfer at Radiant Cooling Surfaces

The heat balance for a radiant cooling surface involves the same heat transfer components as those for other regular interior surfaces. The heat balance equation can be written as follows (Figure 5):

$$q_{surf} = q_{conv} + q_{LWX} + q_{LWS} + q_{SW} + q_{sol} \quad (5)$$

where,

q_{conv}: convective heat transfer at the surface, W/m^2

q_{LWX}: net long-wave radiation exchange between the radiant cooling surface and other zone surfaces, W/m^2

q_{LWS}: net long-wave radiation absorbed from internal loads (e.g., lighting and equipment), W/m^2

q_{SW}: short-wave radiation from lighting absorbed at the surface, W/m^2

q_{sol}: transmitted solar radiation (both direct and diffuse) absorbed at the surface, W/m^2

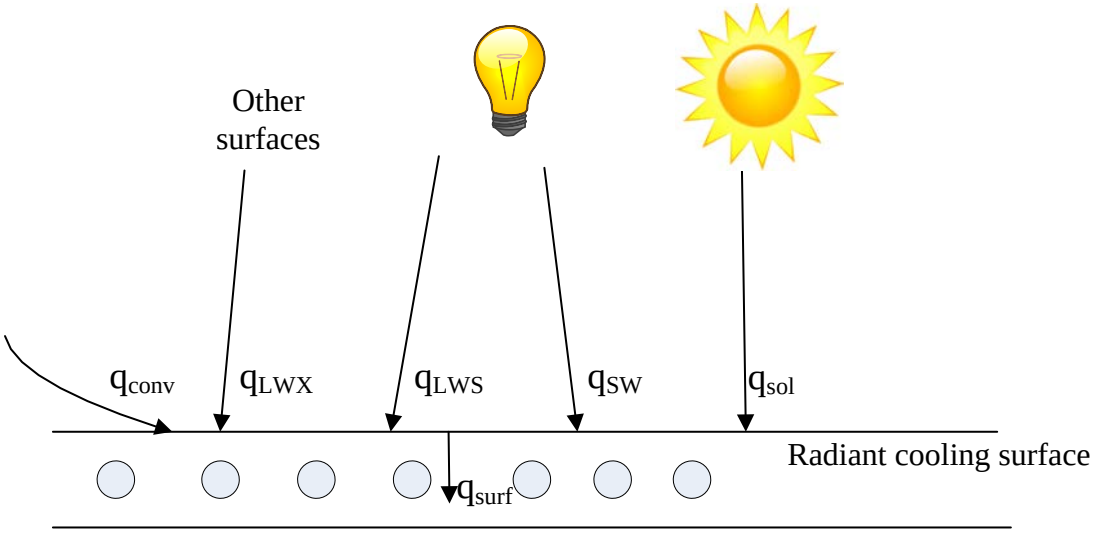

Figure 5: Energy balance at the radiant cooling surface

The last four terms on the right hand side of Eq. 5 are radiation components. As Feng et al. (2013) pointed out, the solar radiation and the radiation exchange with internal loads (i.e., the last three items in Eq. 5) were not given full consideration in design manuals or load calculation procedures for radiant systems. Ignoring these terms may be acceptable for surfaces located in interior zones without solar radiation but will cause an underestimation of the radiant cooling capacity when radiation from solar and internal loads is significant (e.g., perimeter zones).

The surface convective heat transfer can be written as:

$$q_{conv} = h_c(T_{air} - T_{surf}) \quad (6)$$

where, h_c is the convective heat transfer coefficient in W/(m^2 K); and T_{air} and T_{surf} are, respectively, the space air temperature and the radiant cooling surface temperature in °C. The value of h_c varies with surface orientation and the air flow characteristics in the space. The methods used to estimate the surface convective heat transfer coefficients were provided in ASHRAE (2012) and Feng (2014). Empirical correlations for the heat transfer coefficient of a flat plate (representing a floor or ceiling) from Incropera, et al. (2007) revealed that free convection (in the absence of significant air movement), h_c is twice as high for the underside of cold surfaces (ceiling) versus the upper-side of cold surfaces (floor). Thus, locating radiant cooling surfaces on the ceiling increases the convective cooling significantly compared to the floor. A vertical wall has an intermediate value for h_c.

The net long-wave radiation exchange of a cooling surface with other zone surfaces can be written as:

$$q_{LWX} = \sum_j [\sigma F_{surf,j}((T_j + 273)^4 - (T_{surf} + 273)^4)] \quad (7)$$

where, σ is the Stefan-Boltzmann constant of 5.67*10^{-8} W/(m^2 K), T_j is the temperature(°C) of surface j, $F_{surf,j}$ is the radiation exchange factor between the radiant cooling surface with another interior surface j.

For most interior surfaces with conventional materials, Eq. 7 can be approximated as (ASHRAE 2012):

$$q_{LWX} = 5 * 10^{-8} [(AUST + 273)^4 - (T_{suf} + 273)^4] \quad (8)$$

where, $AUST$ is the area-weighted average temperature (°C) of all interior surfaces that can be seen by the radiant cooling surface.

Empirical equations were proposed (Babiak et al. 2009, Feustel and Stetiu 1995) to combine the convective and the net long-wave radiative heat transfer in a simple, linearized manner. The following equations were suggested to calculate the heat transfer between the radiant cooling surface and the space.

For wall cooling:

$$q_{surf} = 8(T_{air} - T_{surf}) \quad (9)$$

For floor cooling:

$$q_{surf} = 7(T_{air} - T_{surf}) \quad (10)$$

For ceiling cooling:

$$q_{surf} = 8.92(T_{air} - T_{surf})^{1.1} \quad (11)$$

Based on Eq. 9 through Eq. 11, the cooling capacity from radiant surfaces can be calculated from the air temperature and the surface temperature. For example, Table 1 shows how the cooling capacity changes with the surface temperature for a space with design air temperature at 24.4°C.

Table 1: Cooling capacities (W/m^2) at different radiant surface temperatures

Construction surface	Cooling surface temperature T_{surf} (°C)				
	18	19	20	21	22
Wall	51.6	43.6	35.6	27.6	19.6
Floor	45.1	38.1	31.1	24.1	17.1
Ceiling	69.3	57.5	46.0	34.8	23.8

It needs to be noted that Eq. 9 through Eq. 11 considers only the heat convection and the long-wave radiation between surfaces. The radiant cooling capacity may exceed 100 W/m^2 if the surface receives direct solar radiation (Babiak et al. 2009).

2.2. 3 Radiant–Based Heating, Ventilation and Air Conditioning (HVAC) Systems

Figure 6 shows a simplified schematic diagram for radiant-based HVAC systems. A plant for cold water generation serves the radiant cooling surfaces in different spaces. An additional system is needed to 1) provide outside air to spaces for ventilation; 2) to address the space latent loads; and 3) to provide

additional sensible cooling to make up the shortage of the radiant system capacity. This section reviews the technology options used for cool water generation and the hybrid HVAC systems.

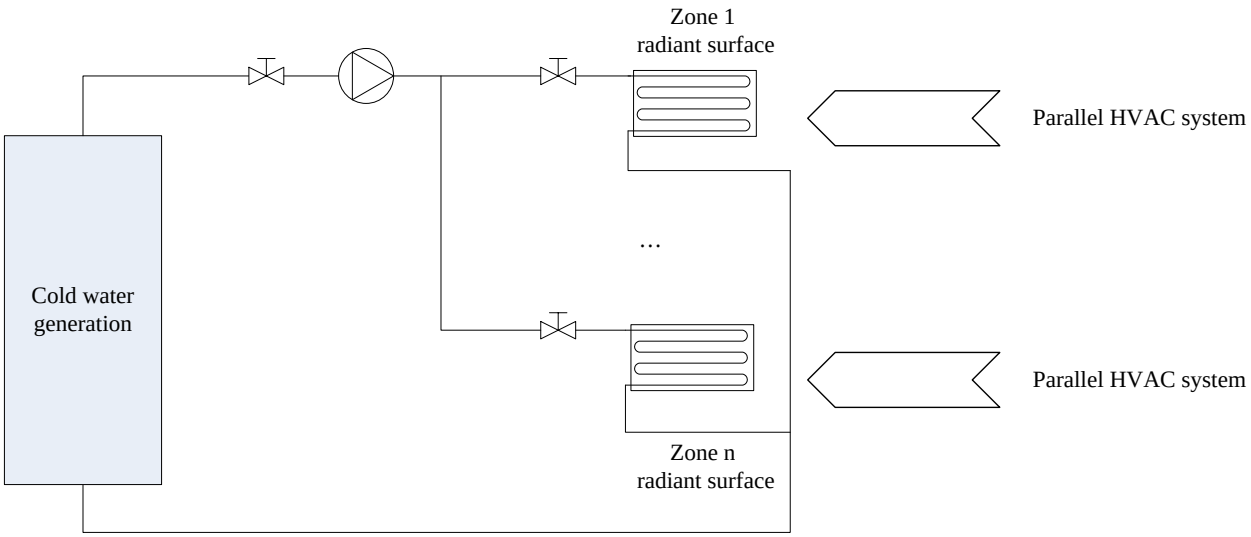

Figure 6: Schematic diagram of radiant-based HVAC systems

Radiant cooling surfaces are operated at a relative higher temperature than the cooling coils in air systems to avoid condensation either on radiant surfaces or within the structure used to embed water pipes. The supply temperature of cold water typically lies in the ranges between 14°C and 20°C. The following sources can be used for high-temperature water cooling (Timothy et al. 2006):

- Chillers. Conventional chillers used in air systems are normally designed for standard conditions with leaving chilled water supply temperature of 6.7°C and entering condenser water temperature of 29.4°C. Chillers can operate more efficiently with the increased chilled water supply temperature. This is especially the case for TABs, which can shift the chiller operation to nighttime when the condenser water temperature can be reduced further. In these situations, variable-speed chillers that can adapt to low-lift operating conditions are more desirable than conventional chillers from an efficiency standpoint. Example projects that use chillers for radiant cooling were reported in Carpenter and Kokko (1998), Hu and Niu (2012), and Sastry and Rumsey (2014).
- Cooling towers (including closed-circuit fluid coolers). Cooling towers can be potentially used as the only source to generate cold water for radiant cooling in the following situations: 1) the space cooling load is low (e.g., in mild climate); and 2) the average wet-bulb temperature during the cooling season is lower than the design supply water temperature. More commonly, cooling towers are used together with chillers for cold water generation. The cooling tower is used as the direct cooling source through water-side economizers for part of the system's operation, when the wet-bulb temperature is low. Using cooling towers for radiant cooling was reported in Bourne and Hoeschele (2000), Doebber et al. (2010), and Vangtook and Chirarattananon (2007).
- Roof-spray evaporative cooling. Bourne and Hoeschele (2000) reported a night roof spray water cooling system, where the cooled water is captured at roof drains and returned through a filter to a storage tank. Tank water is then circulated through in-floor tubing throughout the spray cycle and through zoned fan coils on demand.
- Night-sky radiative cooling. Houghton (2006) presented the design of a 740 m^2 office building using a closed-loop night-sky heat rejection system and a radiant cooling delivery system in slabs. The heat rejection system used solar swimming pool heating panels placed on the roof to take

advantage of the low radiant temperature of the night sky. The cooled water was stored in a water tank and then used during the day to cool the building. The closed-loop design eliminates evaporative water losses. Section 2.1.2 in this report elaborated on the principles and system options for night-sky radiative cooling.

- Ground water or ground source heat pumps. Because of the moderate temperature in the ground all year around, ground source heat pumps can be combined with radiant systems for both heating and cooling. In partial load conditions, ground water can be directly used for cooling through a plate-type heat exchanger rather than running the heat pump. The use of ground source heat pumping for radiant cooling was reported in Budd and Lang (2014, Hu and Niu (2012), Nall (2013a), and Talbot (2013).

A hybrid HVAC system design is almost always needed because radiant cooling alone cannot provide ventilation and address the latent loads (although in some dry climates, it may be sufficient to only address ventilation loads). Some common design options in parallel with a radiant system are reviewed below with a focus on the systems used for ventilation, humidity control, and supplemental cooling capacity. Because this work concentrates on radiant cooling, space heating systems are not covered, although they are usually needed in most buildings.

- Dedicated outdoor air systems (DOASs). A DOAS is often used with a radiant cooling system to provide filtration, heating or cooling, and dehumidification of outdoor air for ventilation. In comparison with conventional air systems, which condition the mixed outdoor and return air to meet both ventilation and thermal comfort, the DOAS has the advantage of more accurate delivery of ventilation to spaces and improved humidity control (Hastbacka et al. 2012). Vapor compression and desiccant cooling are technologies usually found in previous studies for the purpose of dehumidification. Except in mild climates, energy recovery is usually used in DOAS to precondition the outdoor air by exchanging heat with the exhaust air. The combination of DOAS and radiant cooling has been widely studied and adopted in design practice (Armstrong et al. 2009, Doebber et al. 2010, Mumma 2002, Sastry and Rumsey 2014).
- Displacement ventilation (DV). DV provides a low-velocity air stream directly to the occupied zone via diffusers in the wall at floor level or through a raised floor. As the cooler air moves upward, stale and warm air is exhausted from the space at the ceiling level (Hamilton et al. 2004). Because of comfort constraints, the temperature difference between the DV supply air and room air is relatively small (less than 3°C). This low temperature difference and the low air flow rate limit DV cooling capacity. The combination of DV and radiant cooling was discussed in Carpenter and Kokko (1998), Krajcik et al. (2013), Novosela and Srebric (2002), and Zhang et al. (2013).
- Conventional variable-air-volume (VAV) systems. Tian and Love (2009a) reported the use of a VAV system together with radiant slab cooling for a seven-story building. Depending the space condition, the VAV system provides ventilation, space heating, and additional cooling to multiple zones. Such design may complicate the system controls to avoid simultaneous cooling by the radiant slab system and heating by the VAV system.
- Fan coil units (FCUs). Hu and Niu (2012) presented two radiant cooling systems applied in China, which had fan coil units to provide cooling supplemental to the radiant system. Because these fan coil units do not intend to address any latent load, they are called dry FCUs. It is also possible that FCUs are installed to remove humidity of the ventilation air (Nutprasert and Chaiwiwatworakul 2014).

2.2.4 Radiant Cooling System Controls

Similar to conventional air systems, the controls of radiant cooling aim to achieve the desired thermal comfort and energy efficiency. Because of the low-temperature surfaces, condensation control is another major consideration of radiant cooling systems.

Occupants' thermal comfort is affected by several factors including metabolic rate, clothing insulation, air temperature, mean radiant temperature, air speed and relative humidity. Of these factors, the air temperature and the mean radiant temperature are regarded as the most important ones to determine thermal comfort levels in a space. The mean radiant temperature is defined as the uniform temperature of an enclosure, in which the radiant heat loss from the human body is the same as that would occur in the actual (non-uniform) enclosure. If the difference between surface temperatures is small, the mean radiant temperature can be simplified to the following equation:

$$T_{mr} = \sum_i T_i F_{p-i} \quad (12)$$

where, T_{mr} is the mean radiant temperature (°C), T_i is the surface temperature (°C) of surface i, F_{p-i} is the angle factor between a person and surface i.

The combined effects of radiation and convection on occupant's thermal comfort can be evaluated using operative temperature. For a sedentary person not in direct sunlight and in a space with low air velocities (0.2 m/s), the operative temperature can be approximated as the simple average of air and mean radiant temperature:

$$T_{oper} = \frac{T_{air}+T_{mr}}{2} \quad (13)$$

According to ASHRAE Standard 55 (2013), if the air velocity is lower than 0.2 m/s, the operative temperature should range between 24°C and 28°C to satisfy occupant comfort in the cooling season.

Conventional air systems normally use the air temperature set points to achieve the desired thermal comfort. However, because of the lower surface temperature in radiant systems, the air temperature can be reduced to realize the same comfort level as air systems. As Olesen (2008) indicated, for a person sitting at the center of a 6-m by 6-m floor, the angle factor is 0.46 for the floor. Thus, decreasing the floor surface temperature by 5°C has the same cooling effect as decreasing the air temperature by 2°C.

For condensation control, the most important strategy is to limit the radiant system's cold water supply temperature to be higher than the dewpoint temperature of the space air (Nall 2013c). Because a lower air dewpoint temperature allows a lower cold water supply temperature, the space humidity control is highly important to maximize the cooling potential of radiant systems. Acceptable surface temperatures based on comfort and condensation considerations are 19°C for the floor and 17°C for the wall and the ceiling.

Because TABS use building structures for energy storage and shift the cooling load to a different time of day, their control is quite different from other fast-responsive HVAC systems. Nall (2013c) indicated that using an air-temperature-based thermostat to control TABS would likely have less than optimal results, especially if the space is exposed to solar radiation. Based on real building designs, Nall (2013c) presented two general control strategies for radiant slab systems:

- Floor temperature set point reset based on the inside surface temperature of an exterior wall. This strategy applies to buildings or spaces that have exterior envelope with high thermal mass (e.g., concrete block walls). For example, Table 2 shows the reset strategy for a building that has a 0.75-m thick sandstone exterior wall (Nall 2013c).
- Floor temperature set point reset based on the air system operating conditions. This strategy applies to buildings that have the radiant system subordinated to a conventional air system [e.g., a forced air system with an air-handling unit (AHU)]. The control sequence needs to define a deadband of the AHU capacity (e.g., 40% heating and 40% cooling) in which the radiant cooling is inactive. When the cooling output of the AHU varies between 40% and 100% of its cooling capacity, the radiant system is activated and the floor temperature varies between 23.3°C and 20°C. Similar control approaches apply to heating.

Table 2: Radiant floor temperature set point reset based on mass wall inside surface temperature

Wall surface temperature (°C)	Floor temperature set point (°C)
18.8	26.7
19.4	25.0
20.1	23.3
20.8	Off
23.7	Off
24.1	22.2
24.2	21.1
24.4	20.0

On the water side, the cooling capacity can be controlled by configuring the system as a constant flow, variable temperature system or a variable flow, constant temperature system (Strand and Pedersen 2002). Variable flow systems are almost always used in practice because they facilitate individual zone controls (Nall 2013b). In the radiant floor system for a retail building, Doebber et al. (2010) explored the use of a variable flow and variable temperature strategy. Figure 7 shows the variable flow part of the strategy. The radiant floor starts at 20% of the design flow when the space dry-bulb temperature rises to 22.8°C. The same water flow rate is maintained until the space temperature rises to 23.9°C. Then, the flow rate changes linearly in the range between 20% and 100% as the space temperature varies between 23.9°C and 25.6°C. For the variable temperature part of the strategy, the cold water supply temperature is reset based on the radiant system return water temperature, as shown in Table 3 (Doebber et al. 2010). Note that the supply water temperature is relatively low because the building is located in a dry climate and is thus at a reduced risk of condensation.

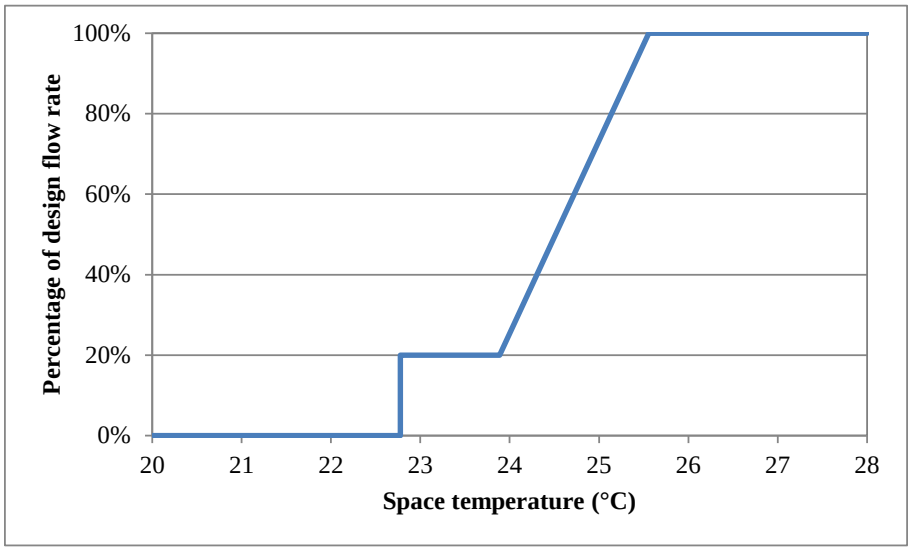

Figure 7: Water flow rate reset strategy for radiant floor cooling in a retail building

Table 3: Cold water supply temperature reset for radiant floor cooling

Return water temperature (°C)	Supply water temperature set point (°C)
≥17.2	12.2
>16.1 and <17.2	12.8
≤16.1	13.3

In addition to the above-mentioned heuristics for radiant system controls, some advanced control methods were proposed in literature. Model predictive control has been increasingly studied in several recent studies (Corbin et al. 2013, Feng et al. 2015, Zakula et al. 2015) to dynamically optimize the operation of radiant slab systems (i.e., TABS).

2.2. 5 Advantages of Hydronic Radiant Cooling Systems

Qualitatively, in comparison with conventional all-air systems, radiant cooling systems have the following major advantages (Olesen 2012, Timothy et al. 2006):

- More energy efficient. The radiant cooling system's energy efficiency comes from the following sources: 1) the radiant system can reduce fan energy significantly because hydronic system can transport a given amount of cooling with less than 5% of the energy required to deliver cool air with fans; 2) the high supply water temperature is beneficial to the operation of vapor compression equipment and expands the potential of using low-grade energy sources for cooling such as evaporative cooling and geothermal energy; 3) the shift of cooling loads to nighttime would further lower the lift of vapor compression equipment and increase the opportunity of free cooling with water-side economizers and night ventilation.
- Improved thermal comfort. The radiant cooling system features a uniform surface temperature close to the air temperature in the conditioned space, reducing the draft impact on occupants.
- Improved indoor air quality. By using a separate air system for ventilation, the radiant system usually eliminates the use of recirculation air that can potentially cause cross-zone contamination. In addition, a dedicated outdoor air system is more accurate and reliable than a mixed air system in delivering the required ventilation to multiple spaces.
- Reduced capital investment. Capital investment of radiant systems may be reduced because 1) the reduced duct size means less space used for duct shafts and a lower plenum height requirement to accommodate ducts; hence, building material cost is reduced; and 2) the HVAC equipment sizes and their initial cost may be reduced because of the shift of cooling loads.

Many studies were made to quantify the energy and cost savings of radiant systems relative to conventional all-air systems. Table 4 below lists the previous work on the comparison between radiant systems and conventional air systems. It can be seem from this table that almost all the work on system performance comparisons was performed through simulation programs. The side-by-side comparison between the VAV system and TABS (Sastry and Rumsey 2014) is an important case study on the savings of radiant systems. In this field comparison, a large office building consists of two identical parts: one part is served by an optimized VAV system while the other part is served by a radiant cooling system (TABS) with DOAS. Over a 2-year monitoring period, the radiant system used 34% less energy than the VAV system.

Table 4: List of previous studies on the potential of energy savings from radiant cooling

Reference	Radiant system type	Baseline system type[1]	Building type	Comparison approach	Climate	HVAC energy savings relative to the baseline[2]
Stetiu 1999	Radiant panel + DOAS	VAV system	Office	Simulation	9 different climates in the US.	17%-42%
Jeong et al. 2003	Radiant panel + DOAS	VAV system	Educational	Simulation	Cold and humid	42%
Armstrong et al. 2009	Radiant panel + DOAS	VAV system	Office	Simulation	5 different climates in the US.	13-18%
Niu et al. 2002	Radiant panel + DV with desiccant cooling	CAV system	Office	Simulation	Hot and humid	44%
Memon et al. 2008	Radiant panel + natural ventilation	Conventio nal air condition-ers	Educational	Simulation	Hot and dry	80%
Tian and Love 2009a	TABS + DOAS	VAV system	Educational	Simulation	Very cold	Up to 80%
Tian and Love 2009b	TABS + DOAS	VAV system	Educational	Simulation	16 different climates in the US.	10% to 40%
Doebber et al. 2010	TABS + DOAS	CAV system	Stand-alone retail	Simulation	Warm and dry	50%
Sastry and Rumsey 2014	TABS + DOAS	VAV system	Office	Measurement	Hot and semi-arid	34%
Henze et al. 2008	TABS + VAV	VAV system	Office	Simulation	Cold and dry	20%
Simmonds et al. 2003	TABS + DV	All air system	Airport	Simulation	Hot and humid	30%
Thornton et al. 2009	Embedded surface systems + DOAS	VAV system	Office	Simulation	16 different climates in the US.	>50%

Note:
1: The baseline system is indicated as conventional air conditioning or all-air system if no specific information on the system is available in the original source. CAV represents constant-air-volume system.
2. A few studies reported the energy savings from a combination of energy efficiency measures.

3. Methodology

The goal of this report is to detail the energy savings that can be expected using an advanced radiative cooling heat exchanger that uses the photonic materials proposed by Raman et al. (2014). This heat exchanger must be considered as part of an overall building and HVAC system design that permits its use and maximizes its potential. To facilitate this analysis, a set of building energy models were developed in EnergyPlus. A typical medium-sized office building was used for the simulation analysis. The selection of this building type is based on the following two major considerations. First, the results obtained from the work can be compared with the previous study (Raman et al. 2014) which used the same medium-sized office building for a rough analysis. Second, the energy savings for office buildings would closely indicate the scale of opportunity in daytime radiative cooling because 1) office buildings account for the largest floor space and energy consumption across the commercial building sector; and 2) many other building types such as outpatient healthcare are similar to office buildings in terms of load profiles, which characterize the primary targeted market for daytime radiative cooling applications.

The building model originated from the building energy codes program (DOE 2015), which maintains a series of EnergyPlus models in compliance with different versions of commercial codes. The building (Figure 8) has three floors and a total floor area of 5000 m^2. The building has a rectangular shape with an aspect ratio of 1.5. Windows are distributed evenly in continuous ribbons around the perimeter of the building. The window fraction of the overall façade area is 33%. The medium office building has steel-framed walls, a flat roof with insulation above the deck, and a slab-on-grade concrete floor. The performance values of the exterior envelope meet the minimum requirement of ASHRAE Standard 90.1-2013 (ASHRAE 2013). More detailed description about the building model including thermal zoning and internal loads can be referred to Thornton et al. (2011).

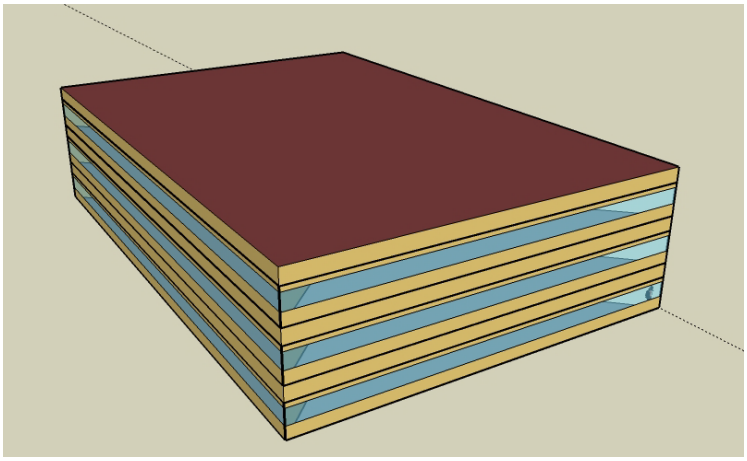

Figure 8: Axonometric view of the medium office building

A reference needs to be established to quantify the potential of energy savings from the photonic radiative cooling system. To make the comparison meaningful, several reference systems are defined as follows:

Reference 1: **VAV system**. This reference is formulated to represent the prevailing technology used to condition medium-sized office buildings. Reference 1 has an individual VAV system for each floor. All equipment types, efficiency, and system design features follow Standard ASHRAE 90.1-2013. The whole building model is essentially the same as the original source (DOE 2015) except for one change. The original model used the mean air temperature to define the heating and cooling set points at 21°C and

24°C, respectively. They were changed to use operative temperature for thermal comfort, with heating set point at 21.6°C and cooling set point at 25.7°C (ASHRAE 2013). Such a change is necessary to make a fair comparison with radiant systems that have a lower surface temperature for cooling and a higher surface temperature for heating. Reference 1 can be used as the baseline representative of conventional air systems meeting the energy standard requirement.

Reference 2: **Hydronic radiant system**. The specification of hydronic radiative cooling requires that the building make use of relatively warm chilled water for cooling. The best available zone-level system design that can accomplish this involves the use of radiant cooling. Reference 2 has hydronic radiant systems for cooling and heating, but without any radiative cooling. The inclusion of this reference allows for an understanding of the marginal benefits of adding radiative cooling.

A diagram of the hydronic cooling system used in the building is shown in Figure 9. A low-lift, air-cooled chiller, described in Section 3.4 provides the source of cooling to a hydronic cooling loop that serves a radiant floor panel in each of the 15 building zones. A variable-speed pump serves this loop and adjusts the flow as necessary to provide sufficient cooling water to all active slabs.

Reference 3: **Conventional radiative cooling system**. Reference 3 builds upon the radiant cooling system from Reference 2, and also includes the specification of a radiative cooling heat exchanger using conventional materials. Such a system could be a lower-cost, competing alterative to a photonic radiative cooling system. The marginal energy savings and economic performance of a photonic radiative cooling system above and beyond Reference 3 should be substantial enough to justify the expected additional cost of the photonic radiator compared to conventional materials. In comparison with the photonic radiative cooler that features daytime cooling, the conventional radiative cooler offers primarily nocturnal cooling. Depending on the characteristics of surface coating on the radiative cooler, two scenarios are considered: Reference 3.1 and Reference 3.2. The former scenario represents the product with the highest solar reflectance index available in the certified cool roof coating database (CRRC 2015). The radiative cooler has solar reflectance of 0.86 and thermal emittance of 0.91. The second scenario represents products with the median solar reflectance index across those white-color metal coatings. In this scenario, the radiative cooler has solar reflectance of 0.65 and thermal emittance of 0.83. Reference 3 can be used as the baseline to obtain the incremental savings from the innovative emittance selective material.

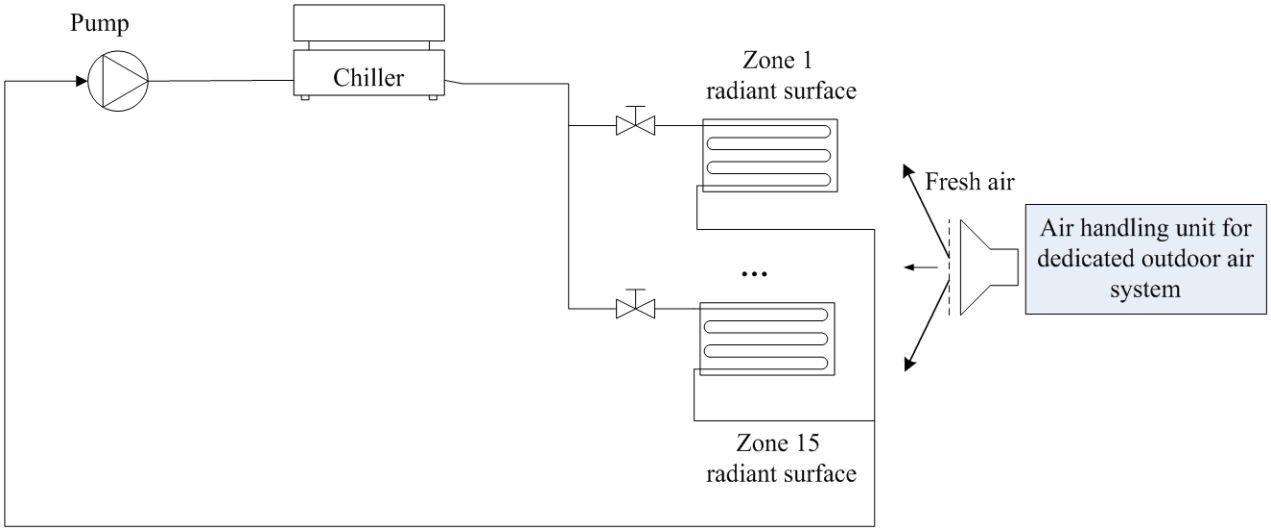

Figure 9: Hydronic system design for Reference 2

The radiative cooling system that was modeled for the photonic radiator and for Reference 3 consists of two hydronic loops, coupled via a cold water storage tank, as shown in Figure 10. A radiative cooling loop circulates water through a roof-mounted radiator via a constant speed pump, drawing water from the cold water storage tank, and delivering water back to the tank. The pump is controlled to run whenever the temperature at the outlet of the radiator is cooler than the temperature of water at the outlet node of the tank within the radiator loop, including the constraint that the loop will not run when the radiator temperature falls below 1°C. Although this loop was modeled as described using water, practical considerations centered around winter freeze-up of the rooftop coils may dictate the use of a glycol-water solution, either for the entire hydronic system, or for the rooftop loop independently. The latter solution would involve the use of a coil within the cold water storage tank to exchange heat. Alternatively, the rooftop loop could be seasonally drained.

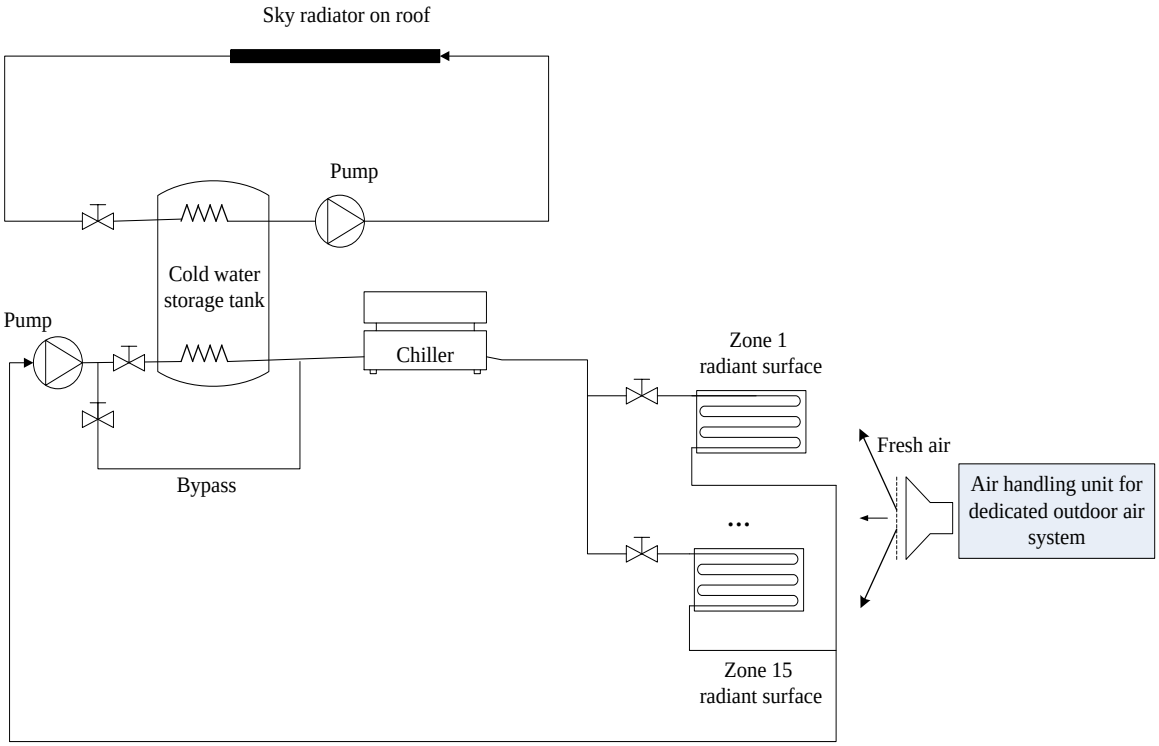

Figure 10: Hydronic cooling loop for Reference 3 and the photonic radiative cooling system

A building cooling loop draws water from the cold water storage tank and sends it to a chiller for final conditioning to the chilled water temperature set point (if necessary). If the tank water temperature at the building loop outlet node from the tank is colder than the chilled water temperature setpoint, the chiller will not be used, and a bypass loop around the tank will temper cold water from the storage tank with relatively warmer water returning from the building to achieve the chilled water temperature setpoint. Chilled water in the building loop is used on-demand when there is a call for cooling from one of the 15 radiant heating/cooling slabs, each embedded in the floor of a building zone. A variable-speed pump serves this loop and adjusts the flow as necessary to provide sufficient cooling water to all active slabs. Components of the system are sized according to Table 5.

Table 5: Hydronic loop component sizing for the radiative cooling systems

Component	Attribute	Sizing	Explanation
Cold Water Storage Tank	Volume	30.96 m^3	Based on modeling of energy savings from conventional radiative cooling, assumed electricity prices and assumed costs of storage tanks, this was determined to be a balanced economical size (where marginal increases in tank size above this point had simple paybacks from energy savings above 10 years).
Radiator Loop Pump	Flow Rate	6.0 L/s	20 kg/h per square meter of the radiative cooler surface area (Eicker and Dalibard 2011).
	Pump Head	2.50 kPa	The calculated pressure drop in each of the parallel pipe segments of the radiator is 1.46 kPa based on the tube diameter, tube length and flow velocity. Some additional pressure drop is assumed as a result of flow entering and exiting the supply and return headers and returning to the tank.
Building Loop Pump	Flow Rate	Autosized by EnergyPlus	
	Pump Head	150 kPa	
Chiller	COP	3.4878	COP at rated test conditions for Daikin low-lift, air-cooled chiller
	Cooling Capacity	Autosized by EnergyPlus	
	Minimum Part Load Ratio	10%	

3.1 Radiator Design

The radiative cooling heat exchanger in Reference 3 is conceptualized as a flat, metallic plate with a surface that is either painted or coated with a high thermal emittance, low solar absorbance finish. Underlying this layer is an array of metallic piping, welded to the underside of the top plate. Each pipe runs parallel from an inlet manifold on one side of the radiator and returns to an outlet manifold on the other side of the radiator. The spacing between pipes is 0.1524 m (6 in.) and the pipe diameter is 0.01905 m (0.75 in.). Water pipes are located in-between the radiative cooler and a thin thermal conductive layer (e.g., aluminum plate). The heat exchanger is assumed to be integrated with the roof construction.

The photonic radiative cooling heat exchanger utilizes the same hydronic piping system and underside connection to the roof; however the surface of the radiator is composed of the deposited microlayer structure described in Raman et al. (2014). The microstructure includes thin titanium and silver layers above a silicon substrate with alternating layers of silicon dioxide (totaling about 1 micron) and hafnium oxide (totaling about ½ micron) in thickness.

To mitigate the convective heat gains from the surrounding, the photonic radiative cooler (Figure 11) is covered with a 25-μm low-density polyethylene film and there is a 2.5-cm air space in between them (Raman et al. 2014). Because mechanical equipment and ventilation infrastructure usually occupy some roof area and because there would likely be a need for corridors to service the radiator, it is not realistic to cover the entire roof with the radiative cooler. Therefore, in this work, the radiative cooler is integrated

with the roof corresponding to the core thermal zone only, which represents about 60% of the total roof area.

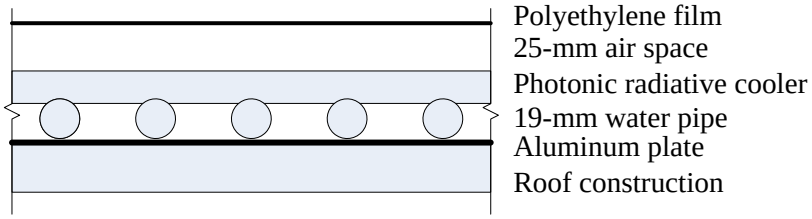

Figure 11: Photonic radiative cooler

3.2 Chilled Water Temperature Control

The chilled water temperature must be controlled to maintain building zones at comfort conditions. To maximize the contribution of radiative cooling, however, the system should be controlled to run at the highest possible chilled water temperature. This minimizes the use of the chiller by bringing the chilled water temperature setpoint closer to the tank water temperature, which has already been maximally pre-cooled by the radiative cooling loop. To achieve a balanced setpoint that meets the cooling needs of the zones while maximizing radiative cooling, a chilled water temperature reset strategy is modeled. The strategy is modeled in energy management system (EMS) and simulates a typical chilled water reset trim-and-respond logic. For each zone, the deviation from the thermostat cooling setpoint is calculated at each timestep. If the average deviation from setpoint is greater than 0.27°C, the chilled water temperature setpoint is decreased at a rate of 2°C per hour. If the average deviation from thermostat setpoint is less than 0.13°C, the chilled water temperature setpoint is increased at a rate of 2°C per hour. Minimum and maximum limits on the chilled water temperature setpoint are set at 12.8°C and 18.3°C, respectively.

3.3 Dedicated Outdoor Air System (DOAS) Design and Control

The dedicated outdoor air system is specified to provide ventilation air to the building in the absence of conventional air-handlers. The DOAS contains a constant volume fan, sized in EnergyPlus to provide 0.4317 L/s of outdoor air for every square meter of floor area. The DOAS system is modeled with an enthalpy wheel that has 68% sensible effectiveness and 61% latent effectiveness, based on an earlier study (Thornton et al. 2009). The enthalpy wheel is controlled to run at a variable speed to target the supply air temperature setpoint from the DOAS system. This helps to eliminate the use of the enthalpy wheel during economizing conditions. A hydronic heating coil and a direct expansion cooling coil provide final conditioning of the supply air from the DOAS system. In Miami, the DOAS supply air temperature setpoint is set to 12.8°C year-round, while in all other climates, an outdoor air temperature-based reset is applied that varies the supply air temperature linearly from 12.8°C at 18°C outdoor air temperature up to 16°C at 10°C outdoor air temperature.

3.4 Chiller Characteristics

An air-cooled chiller is also used to provide auxiliary cooling generation whenever the tank water temperature is higher than the chilled water supply temperature set point. The low-lift chiller from Katipamula et al. (2010) was used here because it is designed for superior performance at part load and "low lift" conditions (reduced difference between the entering condenser air temperature and the leaving chilled water temperature). These conditions are hallmarks of radiant systems, which use much warmer chilled water temperatures than conventional hydronic cooling systems (e.g. 15°C). The chiller has a rated COP of about 3.48. Figure 12 shows the variation of its COP with the condenser inlet air temperature and the evaporator outlet water temperature.

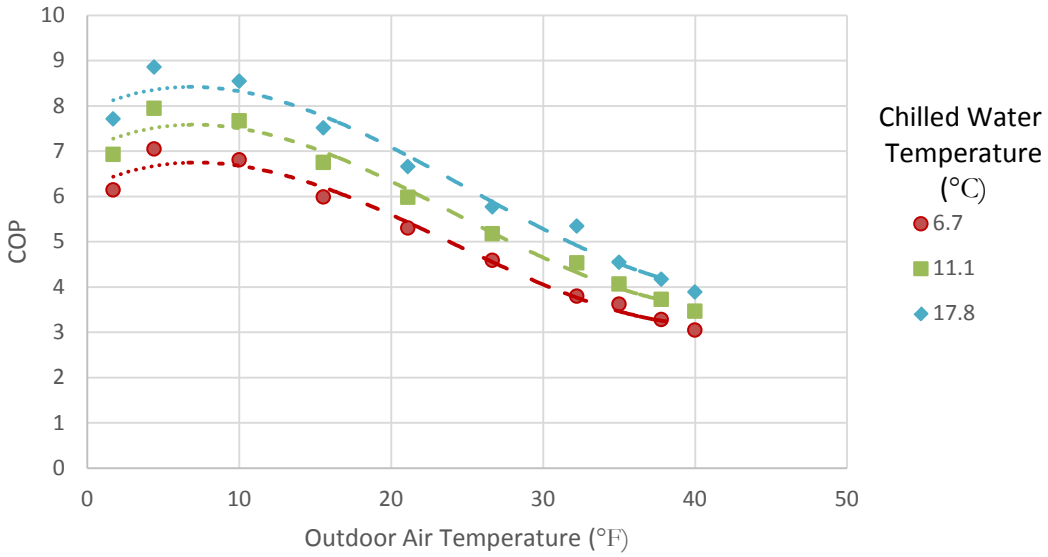

Figure 12: Coefficient of performance of the low-lift chiller

3.5 Heating System

Although not the focus of this work, heating is provided through the radiant floor system as well. A condensing boiler with rated thermal efficiency of 95% is used as the heating source to supply hot water temperature of 45°C.

Because the same radiant cooling slab in each zone is used for both space heating and space cooling, there is the potential for frequent and inappropriate switching between heating and cooling. This can be a problem because the thermal mass of the slab can lead to wasted heating or cooling energy when a previously warmed slab must be cooled (or vice-versa). An outdoor air temperature-based lockout of the zone radiant heat exchangers is used to mitigate this problem. Above 10°C outdoor air temperature, the radiant heating is locked out, and below 15.6°C, radiant cooling is locked out.

3.6 Climate Locations for Simulation

Each of the three reference models, plus the photonic radiative cooling model are simulated in five climate locations, representing four different DOE climate zones. Two marine locations in California (Los Angeles and San Francisco) were modeled, as the combination of relatively cool, dry summer days is expected to benefit radiative cooling, and selecting two locations provides some resolution in terms of the specific benefits in this type of climate. The other three locations are Miami, Florida (hot and humid), Las Vegas, Nevada (hot and dry)_and Chicago, Illinois (warm, humid).

4. Modeling Strategy for Rooftop Radiator

To calculate the expected outlet temperature from a rooftop radiator, as well as the average temperature of the radiator (used as points of intervention by the EMS to the actual model), a discretized heat exchanger was modeled. In a discretized heat exchanger model, a numerical approximation of the heat transfer from a heat exchanger is accomplished by dividing the heat exchanger into a discrete number of segments. In in each segment, the fluid temperature remains constant. This constant temperature assumption allows for tractable calculations of heat flows. The net heat flow into or out of each preceding segment is used to calculate the inlet temperature to the following segment, according to one of two thermal mass equations, depending on whether water is flowing through the heat exchanger or not. When the pump is active and water is flowing through the heat exchanger, water is cooled as it moves sequentially though each segment, and the rate of cooling is governed by the flow rate of water as in Eq. 14.

$$T_{X,t} = T_{X-1,t} + \frac{Q_{net}}{\dot{m} \cdot c_p} \tag{14}$$

$T_{X,t}$ is the outlet temperature of any given segment at the current timestep, while $T_{X,t}$ is the temperature at the inlet of that segment at the current timestep. Q_{net} is the net heating energy absorbed by the segment, $\dot{m}$ is the mass flow rate of water in the segment, and c_p is the specific heat capacity of water.

However, if the pump is off and the water is stagnant in the heat exchanger, the rate of heating or cooling of the water is governed by the mass of water within in the segment and the simulation timestep, dT, according to Eq. 15.

$$T_{X,t} = T_{X,t-1} + \frac{Q_{net} \cdot \Delta t}{c_p \cdot \rho_w \cdot V} \tag{15}$$

where $T_{X,t-1}$ is the node temperature at the previous timestep, Δt is the length of the timestep, ρ_w is the density of water, and V is the volume of the water in each segment, calculated based on the pipe spacing and diameter, and the size of the radiator.

A diagram of the five-segment, discretized heat exchanger that was modeled is shown in Figure 13. The inlet and outlet temperatures from each segment are represented by the numbered T_1 through T_6 temperature nodes. T_1 is equal to the water inlet temperature inlet to the heat exchanger from the storage tank and T_6 is the temperature of the water that returns to the storage tank.

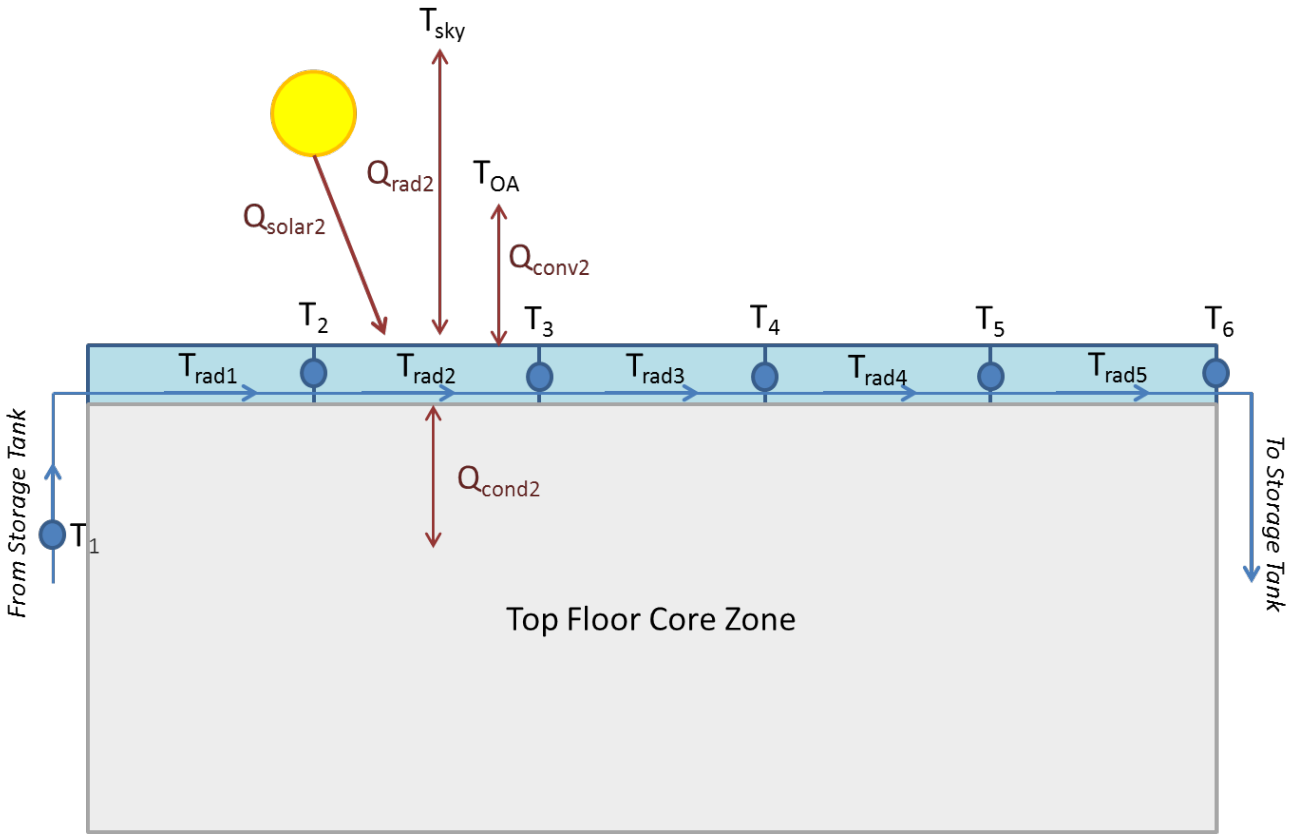

Figure 13: Conceptual diagram of the rooftop radiator, modeled as a discrete heat exchanger.

In Figure 13, the four contributing heat flows to the overall net heat flow into and out of each segment are depicted for one segment (segment 2). These heat flows consist of

- Convection ($Q_{conv,X}$) heat transfer between the upper radiator surface and the ambient air
- Conduction ($Q_{cond,X}$) heat transfer between the underside of the radiator and the underlying building roof
- Net longwave radiation ($Q_{rad,X}$) heat transfer between the upper radiator surface and the sky. This combines the downward radiation from the sky absorbed by the radiator minus the outgoing longwave radiation emitted from the radiator.
- Absorbed solar radiation ($Q_{solar,X}$)

In the calculation of various heat flows, the radiator surface temperature in each segment is estimated as the average of the inlet and outlet temperature to the segment. Because this temperature is being used to calculate the outlet temperature of the segment of the current timestep, calculation of the average of inlet and outlet temperatures for the segment cannot make use of the current outlet temperature ($T_{X,t}$). As an approximation, the outlet temperature from the previous timestep ($T_{X,t-1}$) is used instead. The approximated average temperature in each segment of the radiator in the current timestep is denoted as $T_{radX,t.}$

4.1 Conventional Radiator Materials: Heat Flows

Calculation of $Q_{solar,X}$ relies on EnergyPlus's internal calculations of absorbed solar radiative heat flux on the horizontal surface of the roof. This is impacted by the specified solar absorbtivity of the surface. Two potential surfaces are modeled. One surface, representing a highly favorable cool roof surface has a solar absorptivity of 14%. A second surface with a solar absorptivity of 35% is also modeled.

Calculation of $Q_{cond,X}$ is calculated based on the following thermal conduction equation (Eq. 16)

$$Q_{cond,x} = A_s \cdot k_{roof} \left(T_{zone,t} - T_{RadX,t} \right) \tag{16}$$

where $T_{zone,T}$ is the mean air temperature in the zone directly below the roof, as modelled internally by EnergyPlus, A_s is the total surface area of the radiator segment, and k_{roof} is the thermal conductivity of the roof, as calculated by EnergyPlus (varies by climate zone, according to code-compliant roof constructions)

Calculation of $Q_{conv,X}$ is calculated based on the following convection heat transfer equation:

$$Q_{conv,x} = A_s \cdot h_{roof} \left(T_{amb} - T_{RadX,t} \right) \tag{17}$$

where T_{amb} is the ambient outdoor dry bulb temperature.

h_{roof} is the average convection heat transfer coefficient over the segment, and is calculated based upon correlations developed by Clear et al. (2001) that are applicable to roof surfaces, which are subject to turbulent boundary conditions under typical wind conditions. Two correlations are needed; one is applicable when the radiator surface temperature is colder than the ambient temperature (Eq. 18) and the other when the radiator surface temperature is warmer than the ambient temperature (Eq. 19).

$$h = \eta \frac{k}{L_n 0} 0.15 Ra_{L_n}^{1/3} + \frac{k}{L_{eff}} R_f \, 0.037 \, \mathrm{Re}_{L_{eff}}^{4/5} \, \mathrm{Pr}^{1/3} \tag{18}$$

$$h = \eta \frac{k}{L_n} 0.27 Ra_{L_n}^{1/4} + \frac{k}{L_{eff}} R_f \left[0.037 \, \mathrm{Re}_{L_{eff}}^{4/5} - 871 \right] \mathrm{Pr}^{1/3} \tag{19}$$

In describing each equation, the following four non-dimensional numbers used to express characteristics of fluid dynamics are used: (Eq. 20-23)

$$\text{Reynolds Number: } \mathrm{Re}_x = \frac{w \rho x}{\mu} \tag{20}$$

Where w is the fluid velocity (wind speed in this case), ρ is the fluid density, x is a length term, and μ is the viscosity of the fluid (air). When the Reynolds number is denoted with a different subscript, the content of the subscript is a specific length term and fills in for the x in the equation.

$$\text{Prandtl Number: } \mathrm{Pr} = \mu \frac{\rho}{\alpha} \tag{21}$$

where α is the thermal diffusivity of air, evaluated at the roof film temperature, defined as the average of the radiator surface temperature and the outdoor air temperature.

Grashof Number: $Gr_{L_n} = \frac{g\rho^2 L_n^3 \ \Delta T}{T_f \mu^2}$ (22)

where g is the acceleration due to gravity, 9.81 m/s^2, L_n is the area to perimeter ratio of the roof, ΔT is the difference between the outdoor air temperature and the radiator surface temperature, and T_f is the roof film temperature, in Kelvin.

Rayleigh Number: $Ra_x = \mathrm{Re}_x \ \mathrm{Pr}$ (23)

In Eq. 26 and 27, the first term accounts for free convection and the second term accounts for forced convection. η is a term developed by the authors as a weighting factor for natural convection, based on the non-dimensional Reynolds Number (Re) and Grashof Number (Gr), as shown in Eq. 24:

$$\eta = \frac{\ln\left(1 + Gr_x / \mathrm{Re}_x^2\right)}{1 + \ln\left(1 + Gr_x / \mathrm{Re}_x^2\right)} \quad (24)$$

Here, a limitation of EnergyPlus EMS language was encountered, in that log and natural log math functions are not available. Fixing the size of the roof and the properties of air, an approximate solution was used instead as a function only of wind speed (Eq. 25):

$$\eta = \frac{1}{0.5447w^2 + 0.2315w + 1} \quad (25)$$

k is the thermal conductivity of air, evaluated at the film temperature, R_f is a surface roughness factor, assumed to be 1 for a smooth radiator surface. Finally L_{eff} is a directionally-averaged effective length for forced convection, and is defined as:

$$L_{eff} = (0.938 - 0.056a)b \quad (26)$$

where $a = \frac{4\sqrt{XY}}{2X + 2Y}$ (27)

and $b = \frac{4XY}{2X + 2Y}$ (28)

X and Y are length and width of the horizontal roof.

The net longwave radiation from the radiator surface can be calculated using the Stefan-Boltzmann law:

$$Q_{rad,X} = A_s \sigma \varepsilon (T_{sky}^4 - T_{radX,t}^4) \quad (29)$$

where σ is the Stefan-Boltzmann constant (5.67*10^{-8}), ε is the average spectral and directional longwave emissivity/ absorptivity of the radiator surface, and T_{sky} is the effective sky temperature for longwave radiation, calculated internally in EnergyPlus.

4.2 Photonic Radiator Material: Heat Flows

The photonic radiator proposed by Stanford researchers is modeled using the same framework as described for the conventional radiator, and the same array of piping underlying the radiator surface. The only difference is the surface properties of the radiator itself. The modeling effort for the photonic radiator takes advantage of detailed characterization by the Stanford Researchers of the emissivity of their device as a function of both wavelength and direction of emission.

To calculate the net longwave heat transfer requires integration over three dimensions of space and over all wavelengths of emitted and absorbed electromagnetic radiation. For a given temperature, the total emissivity for a given surface temperature T is given by Eq. 30.

$$\varepsilon(T) = \frac{\int_0^\infty \varepsilon_\lambda(\lambda,T) E_{\lambda,b}(\lambda,T) d\lambda}{\sigma T^4} \tag{30}$$

where $E_{\lambda,b}(\lambda,T)$ is the spectral blackbody emissive power, or in other words, the amount of radiation energy emitted by a blackbody at an absolute temperature T per unit time, per unit surface area, and per unit wavelength λ. It is defined by Eq. 31.

$$E_{\lambda,b}(\lambda,T) = \frac{C_1}{\lambda^5\left[\exp(C_2/\lambda T)-1\right]} \tag{31}$$

where $C_1 = 3.742 \cdot 10^8$ and $C_2 = 1.439 \cdot 10^4$.

The Stanford researchers performed a discretized integration by summing $\varepsilon_\lambda(\lambda,T)$ across an array of measured emissivities at discrete wavelenths and directions. They developed a MATLAB program performs the integration, and also calculates downward absorbed radiation, as a function of T_{amb} and the dewpoint of ambient air, T_d. This allows for a final calculation of net longwave radiation as a function of the radiator surface temperature ($T_{RadX,t}$), T_{amb}, and T_d.

While the integration described above produces the most accurate calculation of net longwave heat flux, approximate values were used in EMS (given its limited computational capabilities), using a regression equation that was applied to the results of the MATLAB calculations. The regression is of the form:

$$q_{rad,X} = a + b\Delta T_{rad} + c\Delta T_{rad}^{\ 2} + dT_{amb} + eT_{amb}^{\ 2} + fT_d + gT_d^{\ 2} + h\Delta T_{rad}T_{amb} + i\Delta T_{rad}T_d + jT_{amb}T_d \tag{32}$$

where $\Delta T_{rad} = T_{amb} - T_{RadX,t}$ (33)

and $Q_{rad,X} = A_s q_{rad,X}$ (34)

The coefficients of Eq. 32 were determined as follows: a=50.93, b= -2.4506, c=0.01359, d= 0.9139, e= 0.005619, f= -0.8513, g= -0.01768, h= -0.0271, i= 0.0000578, j= -0.02216. Figure 14 shows an error analysis for this regression. 95% of the data points used in the regression deviate from the Stanford calculations by less than 2.24 W/m^2.

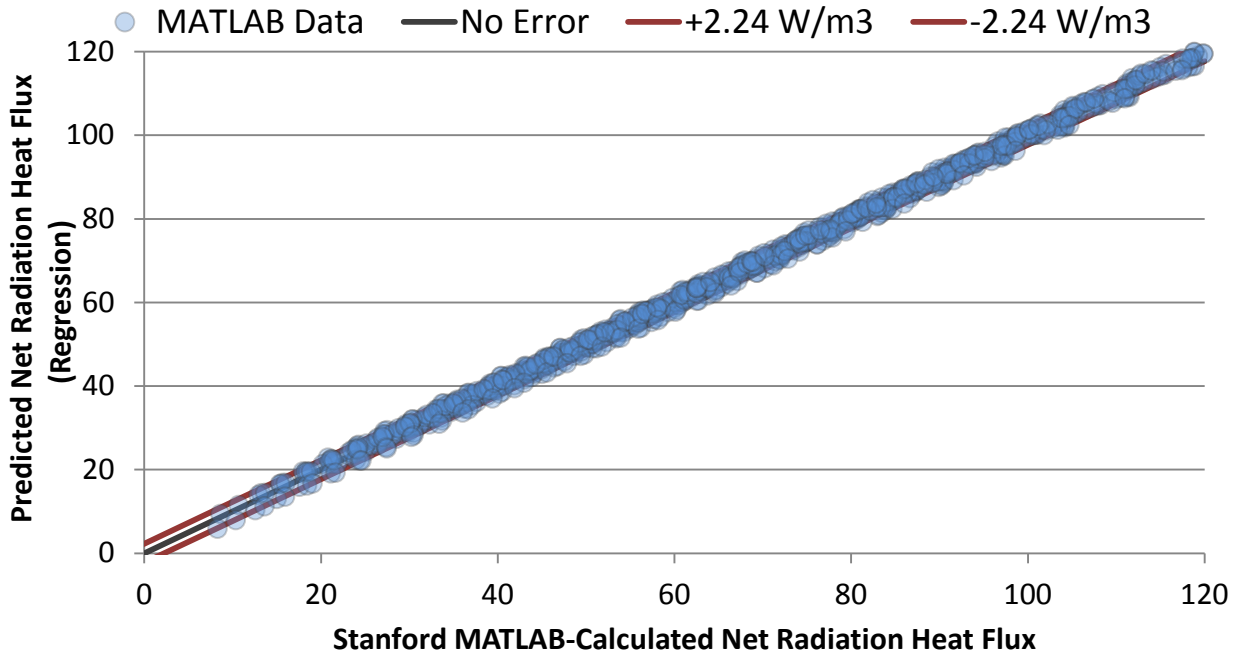

Figure 14: Error analysis for net radiative heat flux for the Stanford photonic radiator

The complete radiator device proposed by the Stanford team differs from the conceptualized conventional radiator (Reference 3) in that it is designed with a transparent cover plate as a convective barrier. According to the researchers, the cover plate is a 25.4-μm thick polyethylene layer, with a solar transmissivity of 92%, and at a distance of 2.54 cm above the radiator surface. To calculate the convective heat transfer from the top of the cover plate to the environment, an assumption was made that the 2.54-cm thick air layer was insufficiently thick for convective air currents to establish. This assumption is bolstered by the fact that the photonic radiator is capable of maintaining a surface temperature below ambient temperature, even when exposed to direct sunlight. Thus, at virtually all times, the air is "stable" inside the cover plate because the lower surface is colder than the upper surface. This means that buoyant forces will keep the air from moving, as the coldest, densest air will settle on the bottom surface. Thus, transfer of heat through the cover plate can be treated as conductive heat transfer, using the conductivity of dry air. This assumption allows for the formulation of a thermal resistance equation (Eq. 35) to calculate the sequential heat flows of conduction through the air gap, conduction through the cover plate, and convection to the ambient air.

$$Q_{conv,X} = A_s \frac{T_{amb} - T_{RadX,t}}{\frac{1}{h} + \frac{\Delta x_{gap}}{k_{air}} + \frac{\Delta x_{cover}}{k_{polyethylene}}} \tag{35}$$

where h is calculated as described for the conventional radiator, but is applied to the convection of air from the top of the cover plate, Δx_{gap} is the air gap thickness, Δx_{cover} is the polyethylene cover thickness, k_{air} is the thermal conductivity of air (0.0257 W/m-k), and $k_{polyethylene}$ is the thermal conductivity of polyethylene (0.33 W/m-k).

Absorbed solar radiation is calculated according to Eq. 44, where the incident solar radiation calculated by EnergyPlus, I_{solar} , is multiplied by the radiator surface's solar absorptivity, α_{solar} (2.5%), and by the solar transmissivity of the cover plate, τ_{cover} (92%). Although α_{solar} and τ_{cover} will vary as a function of solar angle, these relationships are unknown and the constant values are used, as provided by the Stanford researchers.

$$Q_{solar} = A_s I_{solar} \alpha_{solar} \tau_{cover} . \quad (36)$$

Finally, conduction from the underlying roof, $Q_{cond,x}$, is calculated identically to the conventional radiator.

5. Results and Discussion

Simulation results are presented and discussed in this section. First, energy savings of the photonic radiative cooling system are provided. Then, a thermal analysis of the hydronic loop is presented to understand the interactions between different components in Section 5.2. A couple of representative days are used in 5.3 to illustrate the photonic radiative cooler's temperature profiles and cooling energy provision in different weather conditions. A simple economic analysis is made in Section 5.4 to provide a first-order estimation of the minimum acceptable cost for upgrading from the conventional nighttime radiative cooler to a photonic radiative cooler as well as the minimum acceptable cost for a full upgrade from a baseline VAV system design to the photonic radiative cooling system. Finally, a simple analysis is made to investigate the impact of changing from radiant floor slabs to radiant ceilings.

5.1 Energy Savings

The most direct benefit of radiative cooling technology is to save electricity used for cooling. Figure 15 shows the annual cooling electricity consumption for the five system options across all five locations. The cooling electricity was used for both the air-cooled chiller and the DOAS unit. The numbers above the bars indicate the percentage of cooling electricity savings from the photonic radiative cooler relative to the reference system represented by each bar. In Miami, for example, the photonic radiative cooler saved 50% cooling electricity consumption relative to the VAV system and 15% relative to the radiant system. One can observe the following from Figure 15:

- For all five locations, the cooling electricity consumption decreased from the VAV system (Reference 1 in Section 2) to the radiant system (Reference 2) and decreased further for each of the three radiative cooling systems (using the typical nighttime radiative cooler (Reference 3.1), the high-end nighttime radiative cooler (Reference 3.2), and the photonic radiative cooler). A Significant reduction in cooling electricity can be seen from the VAV system to the radiant system for all locations except San Francisco, where efficiency gains are more significantly offset by the elimination of the ability to use the air-side economizer present in the VAV system.
- Relative to the VAV system, the proposed photonic radiative cooling system saved 103 MWh electricity in Miami, 55 MWh in Las Vegas, 50 MWh in Los Angeles, 24 MWh in San Francisco and 43 MWh in Chicago, per year. The saved electricity represents 50%, 45%, 65%, 68%, and 55% of the VAV system's cooling electricity, respectively in the above five cities.
- Relative to the radiant system, which has the air-cooled chiller as the only cooling source for the hydronic loop, the use of photonic radiative cooler saved about 19 to 29 MWh per year depending on the location. The percentage of cooling electricity savings was between 15% and 63%.
- The high-end nighttime radiative cooler saved slightly more cooling electricity than the typical nighttime radiative cooler, but they had very close performance. Relative to the high-end radiative cooler available on the market, the photonic radiative cooler saved 10 MWh electricity in Miami, 13 MWh in Las Vegas, 8 MWh in Los Angeles, 3 MWh in San Francisco and 6 MWh in Chicago, per year, which represents 9%, 16%, 23%, 22%, and 14% of cooling electricity savings, respectively in the above five cities.

The original developers of the photonic radiative cooler made a rudimentary assessment of the electricity savings (Raman et al. 2014) relative to the VAV system. They estimated that the photonic radiative cooler could save about 118 MWh per year in Phoenix, AZ. Because Phoenix and Las Vegas have similar climates, the modeled electricity savings (55 MWh per year) for Las Vegas can be reasonably used for comparison. It clearly shows that the previous work overestimated the saving potential. The overestimation may be caused by the following oversimplifications in (Raman et al. 2014): 1) the radiative cooler surface temperature was assumed to be constant at 24°C; and 2) the cooling power generated from the radiative cooler can be fully converted to space cooling.

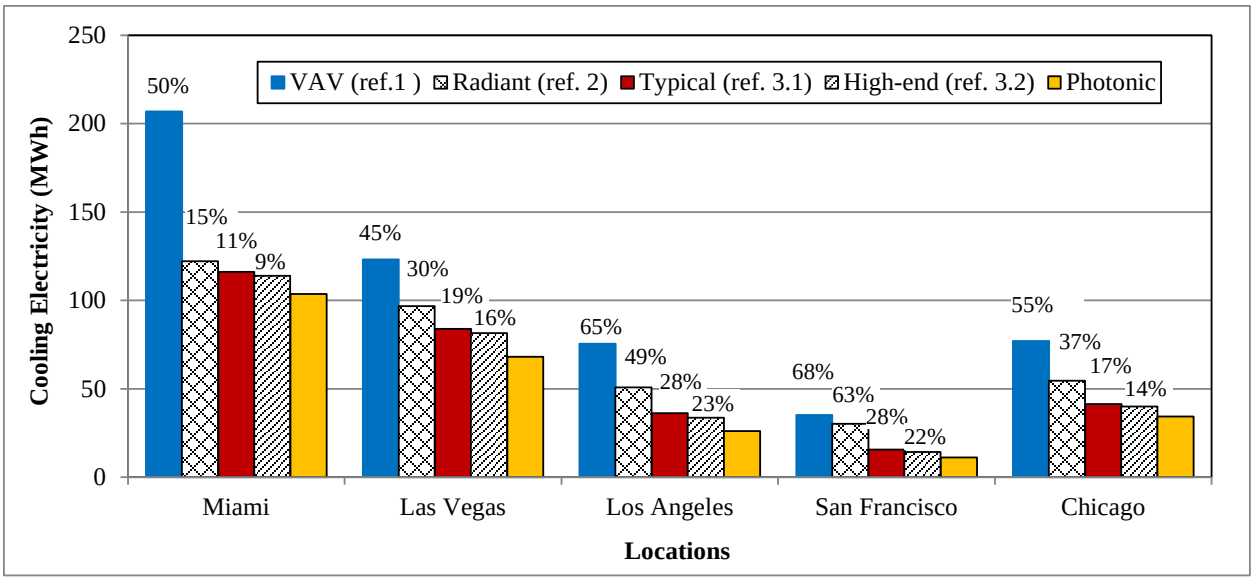

Figure 15: Annual cooling electricity for different systems

In addition to cooling electricity, the use of different systems also affects other energy end uses. For example, relative to the VAV system, all other systems are expected to reduce fan energy and increase pump energy. Therefore, to provide a more complete picture of system performance, Figure 16 shows the combined HVAC energy consumption. Other energy end uses such as lighting and plug loads are identical for all systems and they are not presented here. The pattern of changes in HVAC energy uses between different systems is similar as those for cooling electricity in Figure 15, although the percentages of savings become smaller because of the larger denominator (HVAC energy vs. cooling electricity). Figure 16 reveals that the photonic radiative cooling system reduced HVAC energy by between 29% and 62% relative to the VAV system and only 2% to 14% relative to the high-end nighttime radiative cooler.

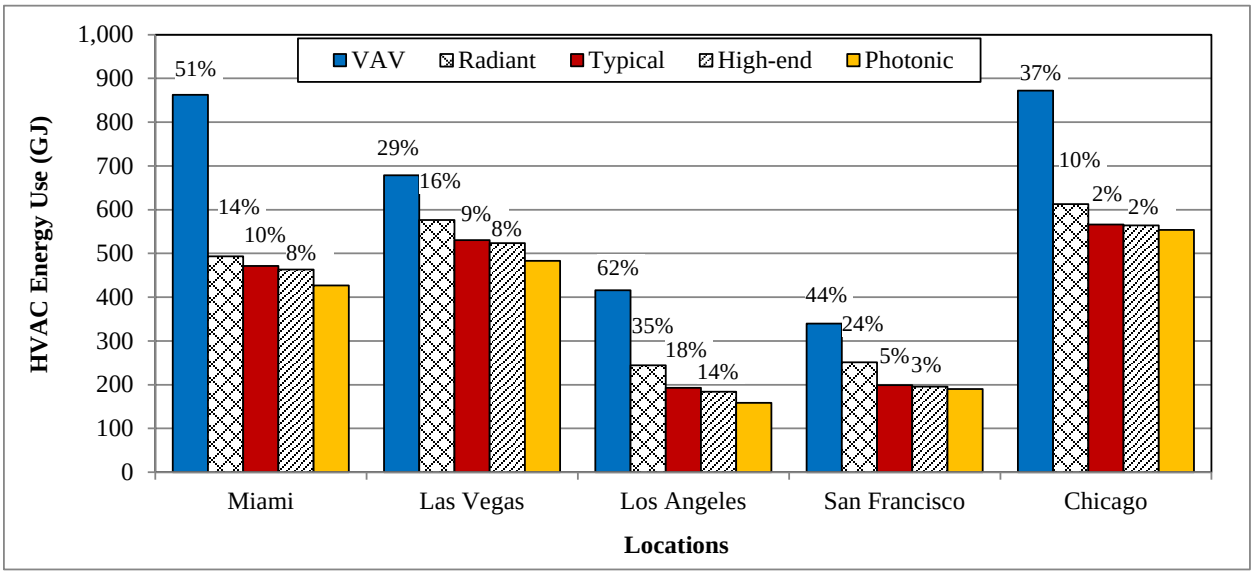

Figure 16: Annual HVAC energy consumption for different systems

5.2 Thermal Analysis of the Hydronic Loop

As Figure 10 shows, the water returned from radiant floors gets cooled by the storage tank or the air-cooled chiller. The tank cooling energy is from the radiative cooler, so it can be regarded as "free" energy. For the photonic radiative cooling system, the percentage of free energy used to address the cooling load is illustrated in Figure 17 for each month in all five locations. This figure shows the following:

- As expected, the percentage of free cooling was less in summer, when there was a higher cooling load and a lower radiative cooling potential.
- The supplementary air-cooled chiller must be used in Miami for all 12 months. In Las Vegas, Los Angeles, and Chicago, the radiative cooler was sufficient to meet the cooling load in the coldest 5 months of the year. In San Francisco, free cooling was sufficient to meet nearly the entire cooling load year-round.
- In the cooling season (June to September), the free energy addressed about 10% of cooling load in Miami, between 17% and 36% in Las Vegas, between 61% and 84% in Los Angeles, more than 90% in San Francisco, and between 26% and 63% in Chicago. Although Las Vegas and Los Angeles belong to the same climate zone (ASHRAE 2013), the latter had far more radiative cooling potential because of lower sky temperatures in Los Angeles.

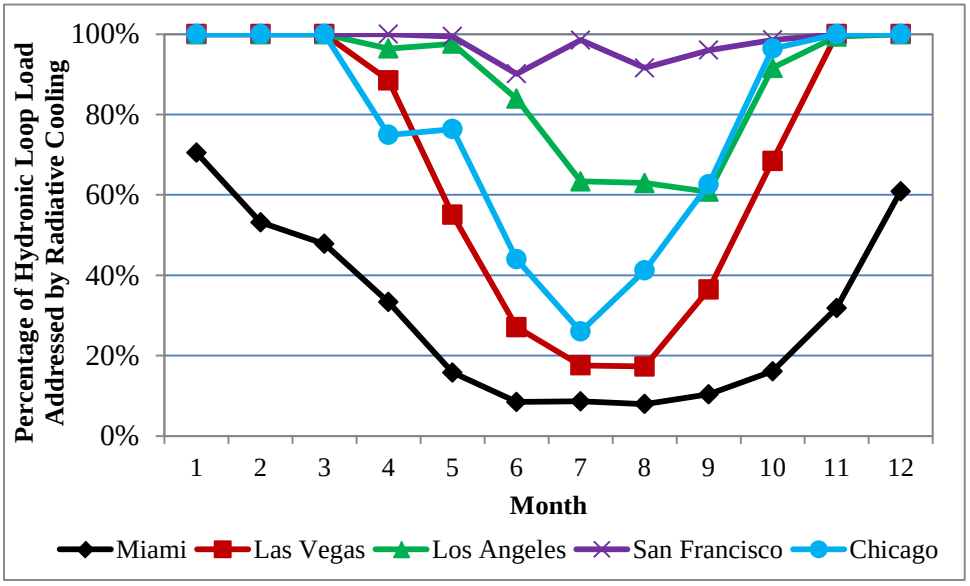

Figure 17: Monthly percentage of the hydronic loop cooling load addressed by photonic radiative cooling across the whole year in the considered five locations.

Figure 18 shows the percentage of free energy used to address the hydronic loop cooling load for the nighttime radiative cooling system with the high-end product (Reference 3.2). In contrast to the photonic radiative cooler, the high-end nighttime radiator had much less cooling capability. In the summer (from June to September), the percentage of the hydronic loop cooling load that was addressed by free radiative cooling decreased by between 20% and 40% relative to the photonic radiative cooler.

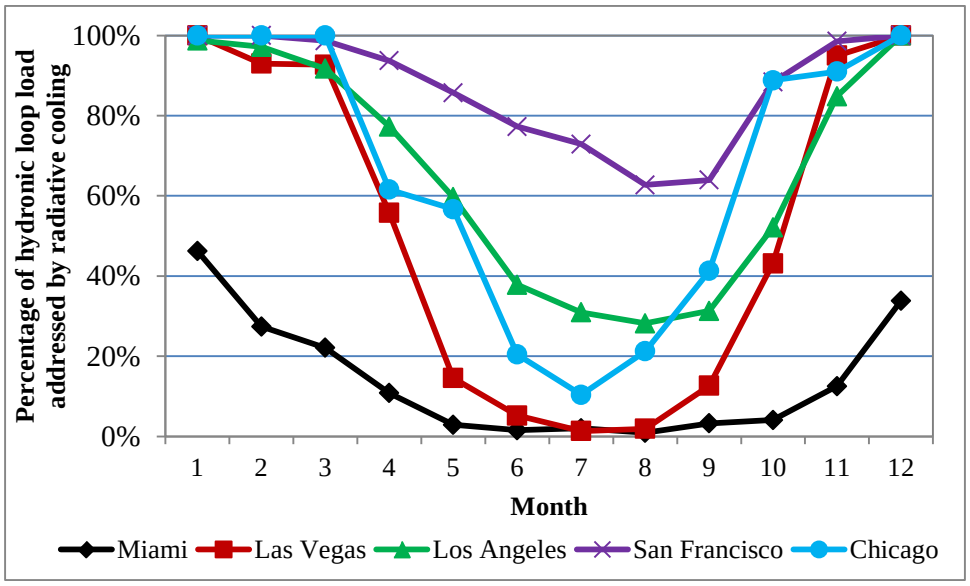

Figure 18: Monthly percentage of the hydronic loop cooling load addressed by high-end nighttime radiative cooling across the whole year in the considered five locations.

In general, radiative coolers provide more cooling energy during the nighttime than during the daytime. Because of the asynchronization and imbalance between radiative cooling generation and space cooling loads, the cold water tank plays an important role to store the cooling energy generated at night for daytime use. Figure 19 shows the annual energy charged to and discharged from the tank over daytime and nighttime for the photonic radiative cooler. The findings are the following:

- Daytime charging accounted for a significant portion of the overall energy charged to the tank. Our calculation indicated that daytime contributed 30% of the annual energy charge in Miami, 51% in Chicago, and about 37% in each of the other three locations.
- In all locations, the overwhelming majority of energy discharged from the tank occurred during the daytime when the cooling load was high. About 90% of the annual energy discharged from the tank in Miami and over 95% discharged in each of the other four locations occurred during the day.
- Because of tank skin losses to the surroundings, the energy discharged from the tank was slightly less than the energy charged to the tank. The cycling efficiency was calculated to be about 95% for all locations.

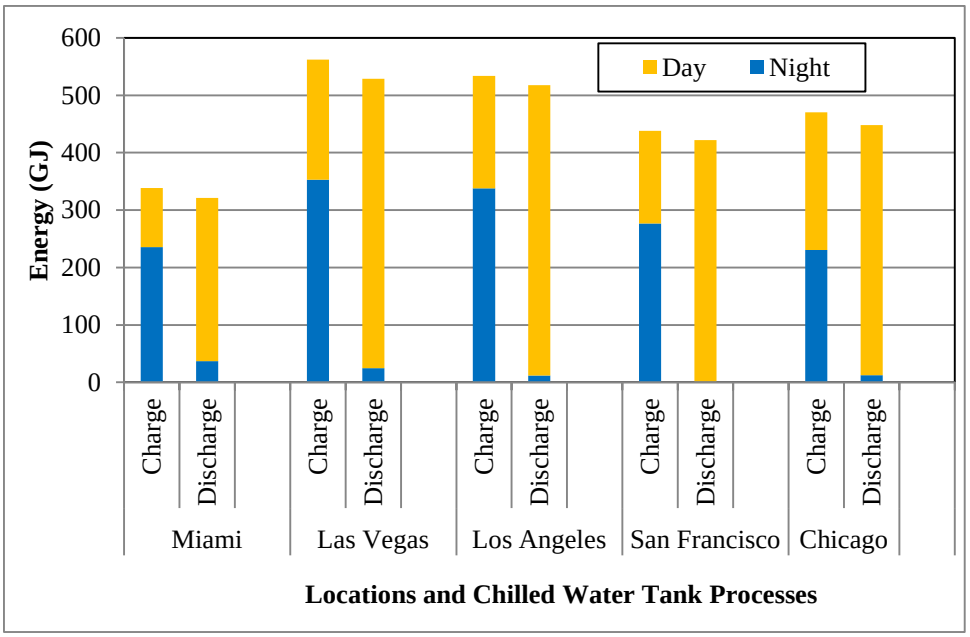

Figure 19: Comparison of annual energy charging to and discharging from the storage tank between day time and nighttime

Figure 20 compares the novel photonic radiative cooler and the high-end nighttime radiative cooler in the market with regard to the magnitude of energy charged to the water tank. We can draw the following conclusions from this figure:

- The photonic radiative cooler charged 340 GJ, 560 GJ, 530 GJ, 440 GJ, and 470 GJ cooling energy per year to the tank, respectively in Miami, Las Vegas, Los Angeles, San Francisco, and Chicago. For the high-end conventional radiative cooler, the total charged energy was reduced to 150 GJ, 330 GJ, 380 GJ, 390 GJ, and 360 GJ for the same five cities. The photonic radiative cooler provided 123%, 69%, 40%, 13%, and 30% more free cooling energy than the conventional radiative cooler, respectively in the above five locations.
- After normalization with the radiative cooler area, the annual free cooling density achieved by the photonic radiative cooler varied between 344 MJ/m^2 in Miami and 570 MJ/m^2 in Las Vegas. For the high-end nighttime radiative cooler, the annual free cooling density varied between 154 MJ/m^2 in Miami and 395 MJ/m^2 in San Francisco.
- The photonic radiative cooler provided significantly more free energy during the daytime than the conventional radiative cooler, which demonstrates the desired daytime cooling potential from the novel technology. The difference was particularly evident in Miami, Las Vegas, and Los Angeles. In contrast, the conventional radiative cooler generated the predominant portion of its free cooling energy at night

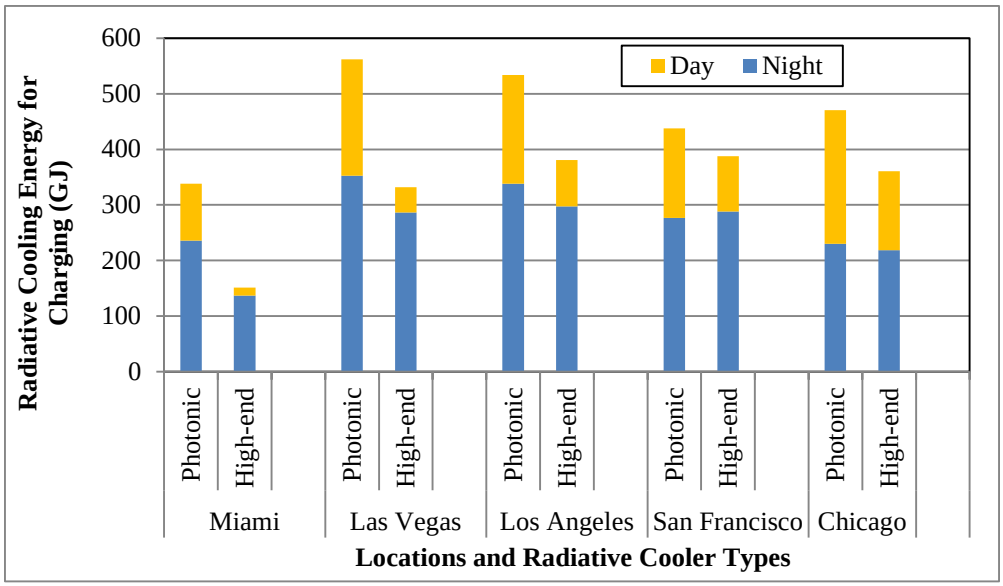

Figure 20: Comparison of annual energy charging during day and night between the photonic and the high-end nighttime radiative coolers

5.3 System Operation in Selected Representative Days

Figure 21 shows a graph of key system node temperatures and energy flows during a 2-day period during the shoulder season (April 24-25) in Las Vegas. These 2 days are in the middle of the work week. The outdoor air temperature (gray, dotted line) varies from a morning low of 17.5°C at 4:00 a.m. to a high of 26.4°C at 3:00 p.m. on April 24, and varies from a morning low of 15.6°C at 6:00 a.m. to a high of 26.7°C on April 25. The radiator surface temperature at the outlet of the radiator (red line) remains well below the ambient air temperature during this period, averaging 9.2°C below ambient at the radiator outlet. Because the radiator outlet temperature remains below the cold water tank's charge outlet node temperature (purple line), water flows through the radiator (charges the tank) the entire period. The green bars (right axis) show the magnitude of cooling energy being charged over this period. The peak charging occurs in the late evenings, following periods of rapid decline in outdoor air temperatures. At this time of day, the tank water is relatively warm and thus has a greater potential to be cooled. The chilled water temperature set point remains in the warmer end of the reset range (15 to 18.3°C; dark blue line), because of moderate demands for chilled water from the radiant panels. This makes free cooling easy to achieve at most hours using only tank water. The cold water tank's use side outlet node temperature is well below the chilled water temperature set point during morning start-up on the first day (dropping to as low as between 5 and 6°C at 6:00 a.m. on April 24) and provides all of the cooling for the building (light blue bars). The tank water gradually warms as it is drawn off for space cooling during the day. By 2:00 p.m. on April 24, the tank water temperature rises above the chilled water temperature set point, and the chiller comes on to supplement the tank water (dark blue bars), which at that time is still providing a significant fraction of the cooling. By 4:00 p.m. on April 24, the use side outlet temperature is at about the same temperature as the return water from the building (orange line), and thus provides no additional cooling benefit. Until the building becomes unoccupied at 6:00 p.m., the chiller meets the entire cooling load. The same general pattern plays out the following day. During this 2-day period, radiative cooling

provides 81% of the building's chilled water cooling demands, while the chiller meets the remaining 19%.

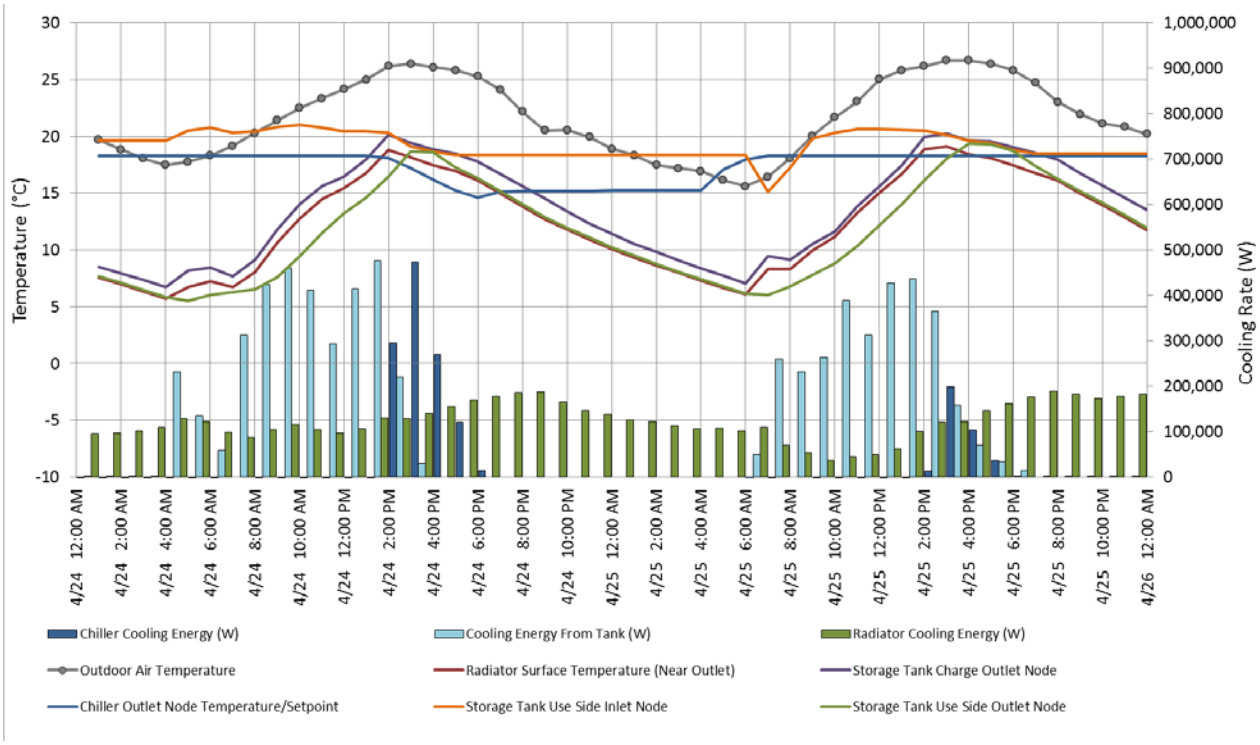

Figure 21: Shoulder season operation of the radiative cooler, storage tank and chiller in Las Vegas, NV

Figure 22 shows a graph of key system node temperatures and energy flows during a 2-day period during peak summer conditions (July 13-14) in Las Vegas. Low temperatures during this period are around 29°C, while high temperatures are between 40 and 43°C. The radiator surface temperature remains well below the ambient temperature the entire period, averaging 15.3°C below the ambient temperature. This is a much improved temperature drop compared to the shoulder season, yet because of the extreme heat, there are only limited periods where tank charging is possible. These periods are limited to nighttime hours with peaks in the early mornings. The reason for the reduced charging of the tank is that the radiator surface temperature remains above the tank water temperature at the charge outlet node whenever outdoor air temperatures are above roughly 35°C. Because of high demands for chilled water in the building, the chilled water temperature set point remains at the low end of the reset range (generally between 12.8 and 14°C), except during the early morning hours. This low temperature set point makes it even more challenging for the radiative cooler to contribute towards cooling of the building's chilled water loop. On both mornings, there is a 3-hour period from 5:00 a.m. to 7:00 a.m. where the building is being cooled from tank water alone. By 9:00 a.m. both mornings, the chiller is providing 100% of the cooling. Overall, the radiative cooler provides only 12% of the building's cooling demands over this 2-day period.

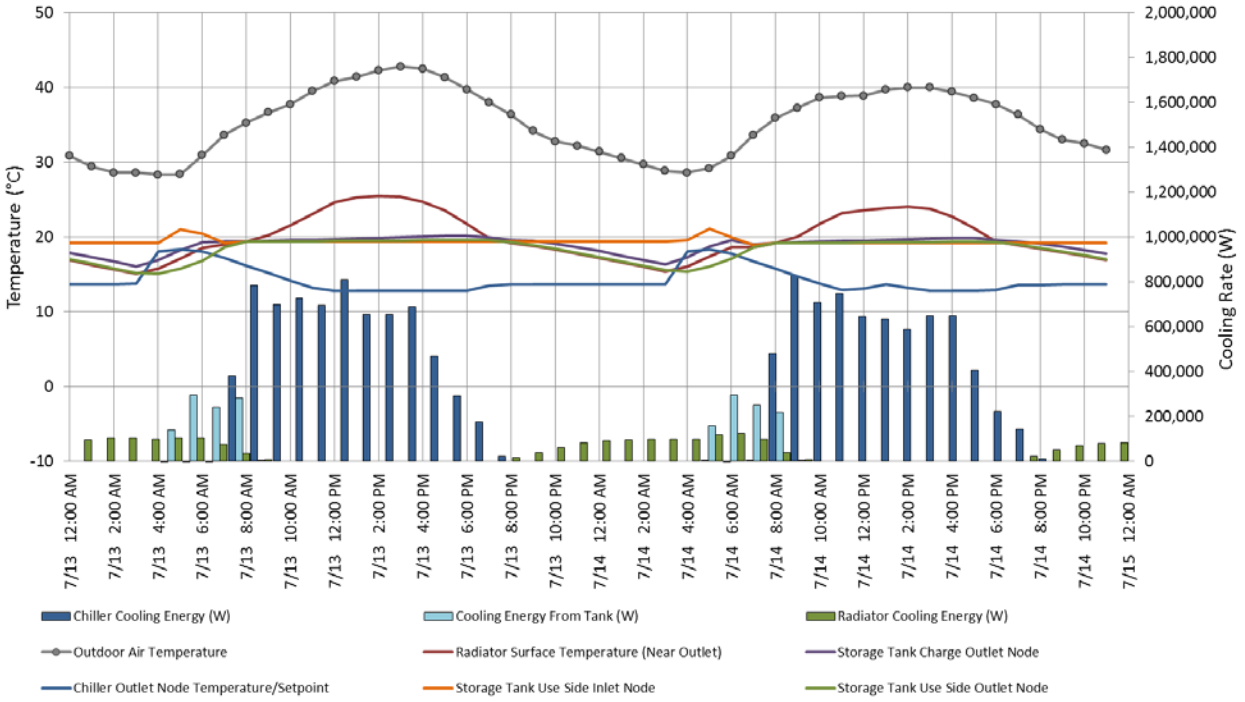

Figure 22: Peak summer operation of the radiative cooler, storage tank and chiller in Las Vegas, NV

5.4 Economic Analysis

The photonic radiative cooling technology evaluated in this work is still in the stage of research prototype development. The initial cost of such photonic radiative coolers after commercialization is unknown. Thus, it was not feasible to calculate the simple payback based on initial costs and energy bill savings. To address this, we calculated the maximum acceptable cost increase relative to commercial products to achieve a specific simple payback period. Average blended electricity prices from the U.S. Energy Information Administration (EIA 2015) were used for the analysis. According to EIA, the 2013 average retail prices of electricity in the five locations are 8.56, 9.22, 13.82, 16.33, and 8.54 cents per kWh, respectively. The photonic radiative cooling system and the Reference system 3.2, which uses the high-end commercial product for nighttime cooling, have different cooling electricity consumption while other energy end uses are identical or have negligible difference. Thus, based on the cooling electricity consumption shown in Figure 15, the maximum acceptable incremental cost relative to the high-end commercial product was calculated as:

$$IC = \left(Elec_{HighEnd} - Elec_{Photonic}\right) * r_{elec} * Y/A \quad (37)$$

where, IC is the maximum acceptable incremental cost in \$/m^2 , $Elec$ indicates annual electricity consumption in kWh, r_{elec} is the electricity price in \$/kWh; Y is the simple payback period in years; A represents the radiative cooler area, which is equal to 984 m^2 in this case.

Figure 23 shows the calculated acceptable incremental cost of the photonic radiative cooler in five locations. This figure indicates that for a given simple payback period, the acceptable incremental cost is highest in Las Vegas and lowest in San Francisco and Chicago, which have almost identical acceptable costs. The acceptable incremental cost ranged from \$0.5/m^2 to \$1.25/m^2 for 1-year simple payback, from \$1.5/m^2 to \$3.75/m^2 for 3-year simple payback, and from \$2.5/m^2 to \$6.25/m^2 for 5-year simple payback. This analysis, however, does not account for climates in which radiative cooling using conventional

materials is not cost effective in the first place – and thus an incremental improvement to photonic radiative cooling may be irrelevant.

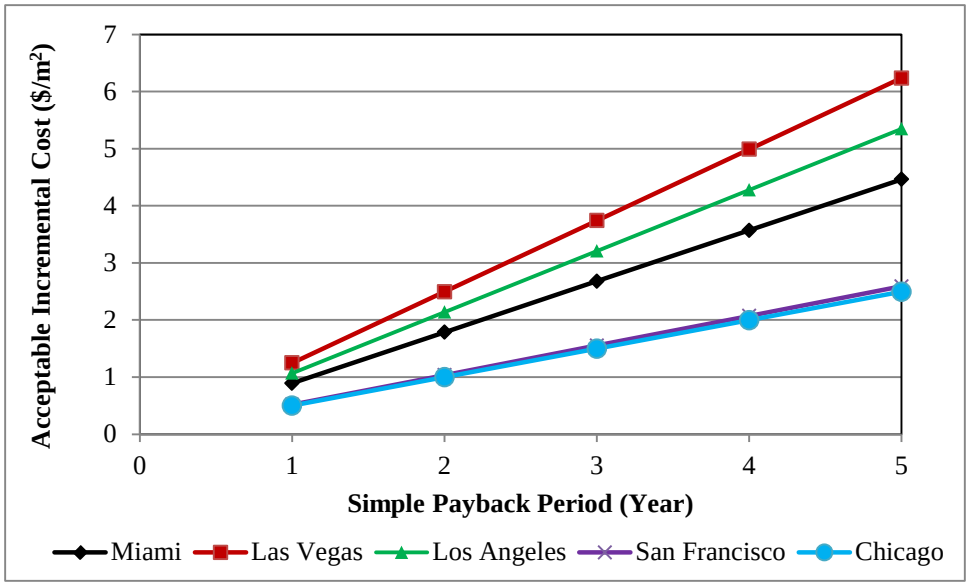

Figure 23: Maximum acceptable incremental cost per unit area of a photonic radiative cooler as an upgrade from a high-end nighttime radiative cooling product to achieve the desired simple payback periods

Similar economic analysis was also made for the full upgrade from the VAV system to the photonic radiative cooling system. Because this system upgrade involves the change of natural gas consumption for heating, the latest natural gas prices were obtained from EIA (2015), which are 1.14, 0.82, 0.91, 0.91, and 0.89 dollars per therm, respectively, in the five locations. Instead of using the radiative cooler surface area, the incremental cost was normalized by the building space area because the system changes are far beyond the scope of radiative cooling heat exchanger itself. For the photonic radiative cooling system, the maximum acceptable incremental cost relative to the VAV system was calculated as:

$$IC = \{(Elec_{VAV} - Elec_{Photonic}) * r_{elec} + (NG_{VAV} - NG_{Photonic}) * r_{gas}\} * Y/A_{bldg} \quad (38)$$

where, $Elec$ and NG, respectively, refer to annual electricity consumption (kWh) and annual natural gas consumption (therm); the subscripts VAV and $Photonic$ refer to the VAV system and the photonic radiative cooling system, respectively; A_{bldg} represents the building area, which is equal to 4982 m^2 in this case.

Figure 24 shows the calculated results on the acceptable incremental cost for the system upgrade from VAV in five locations. This figure indicates that for a given simple payback period; Las Vegas has the minimum acceptable incremental cost while the other three locations have very close acceptable incremental costs. The acceptable incremental cost ranged from \$1.8/m^2 to \$2.3/m^2 for 1-year simple payback, from \$5.0/m^2 to \$6.9/m^2 for 3-year simple payback, and from \$8.3/m^2 to \$11.5/m^2 for 5-year simple payback.

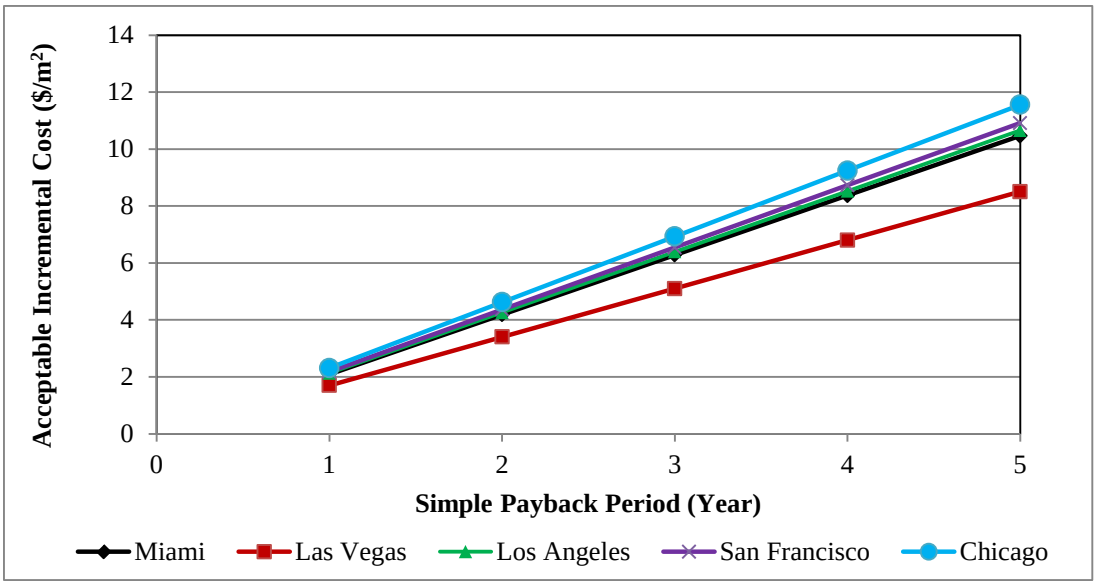

Figure 24: Maximum acceptable incremental cost per unit area of building space as an upgrade from the VAV system to the photic radiative cooling system to achieve the desired simple payback periods

5.5 Sensitivity Analysis on Radiant Surfaces

Recall that floor slabs were used as the radiant surfaces in all systems except for the VAV system. In addition to radiant floor slab systems, the ceiling is another potential location for use as the radiant surface. This may have benefits for cooling because of the advantage of enhanced convective heat transfer from the ceiling. To investigate the impact of radiant surfaces on energy use, we placed the water tubes in the bottom part of the floors to approximately model capillary mats embedded in the plaster or gypsum layer of the floor construction. Figure 25 compares the annual cooling electricity consumption between the systems using radiant floor slabs and those using radiant ceilings, while Figure 26 compares the annual HVAC energy use. These two figures show that for the same system type, radiant ceilings have less cooling electricity consumption than radiant slabs. The same observation generally applies to annual HVAC energy use except for the radiative systems in San Francisco, which have slightly more energy use from radiant ceilings when combined with radiative cooling.

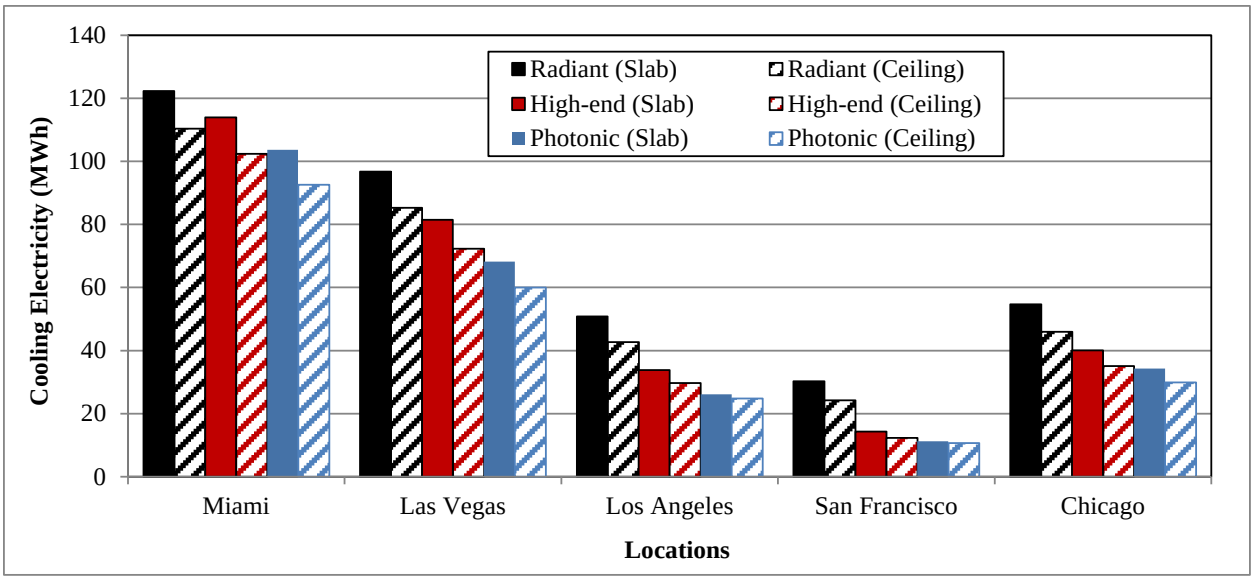

Figure 25: Comparison of annual cooling electricity between the systems using radiant slabs and those using radiant ceilings

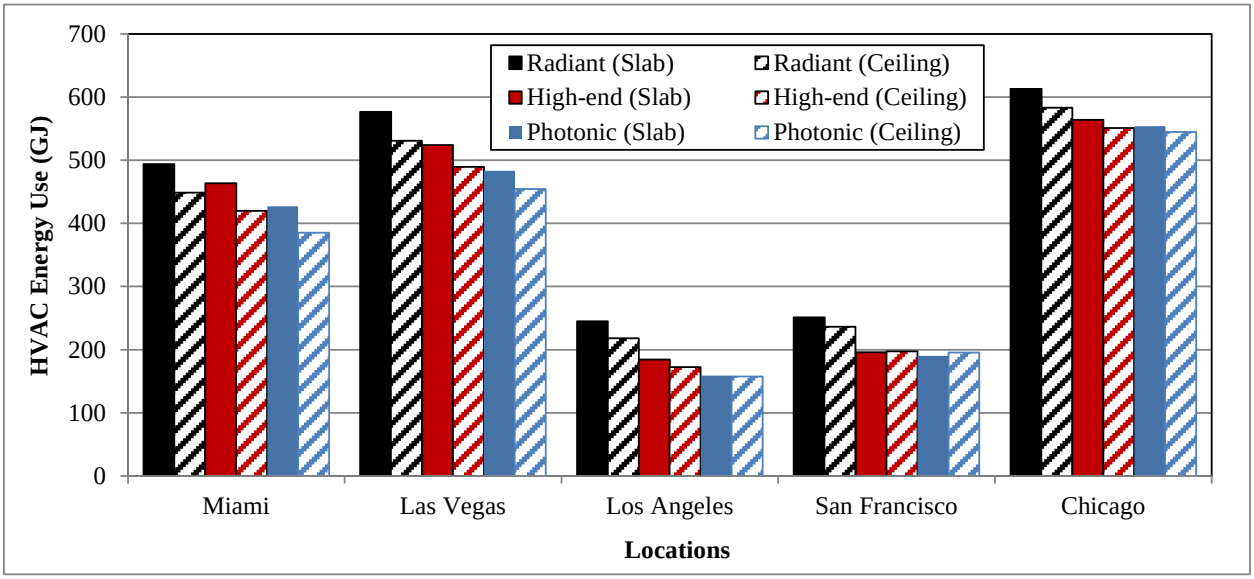

Figure 26: Comparison of annual HVAC energy use between the systems using radiant slabs and those using radiant ceilings

Although the radiant ceiling system consumes less energy than the radiant slab system, the energy savings of the photonic system relative to the radiant system or the nighttime radiative cooling system does not increase if the radiant surfaces change from the floor slab to the ceiling. Figure 27 and Figure 28, respectively, show the percentage savings of cooling electricity and HVAC energy use. In these two figures, each bar indicates the percentage of savings of the photonic system with same radiant surfaces as the baseline system represented by each bar. The savings percentages are close in some locations (e.g.,

Las Vegas and Chicago) but using slabs as the radiant surfaces leads to higher savings percentages in some locations (e.g., Los Angeles and San Francisco).

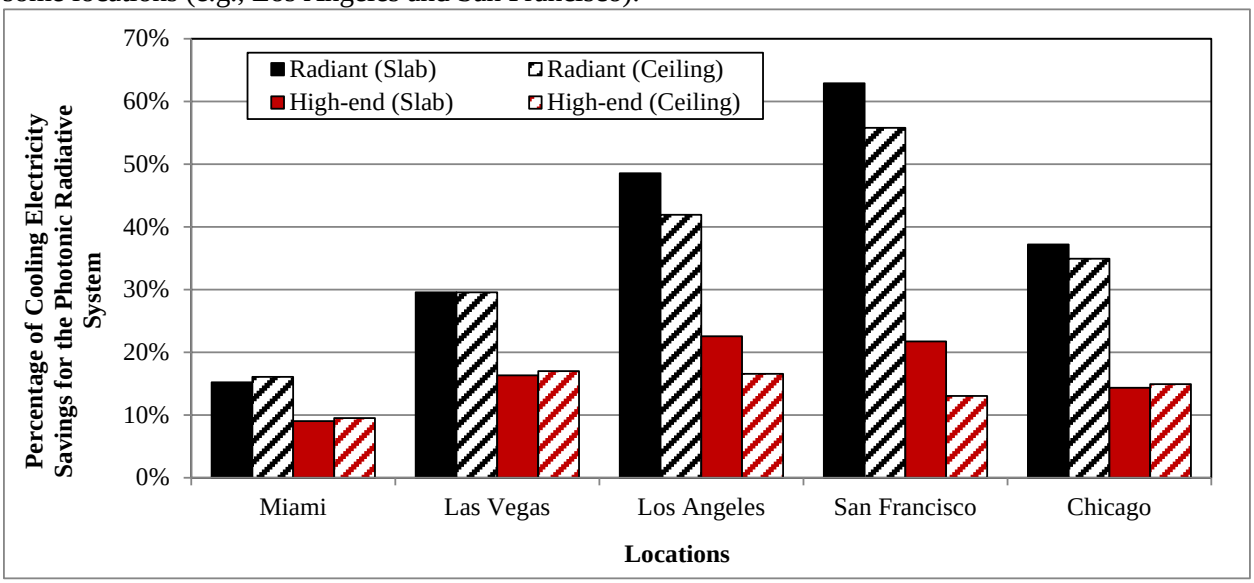

Figure 27: Cooling electricity savings (percent) from the photonic system relative to the radiant system (Reference 2) and the high-end nighttime radiative cooling (Reference 3.2)

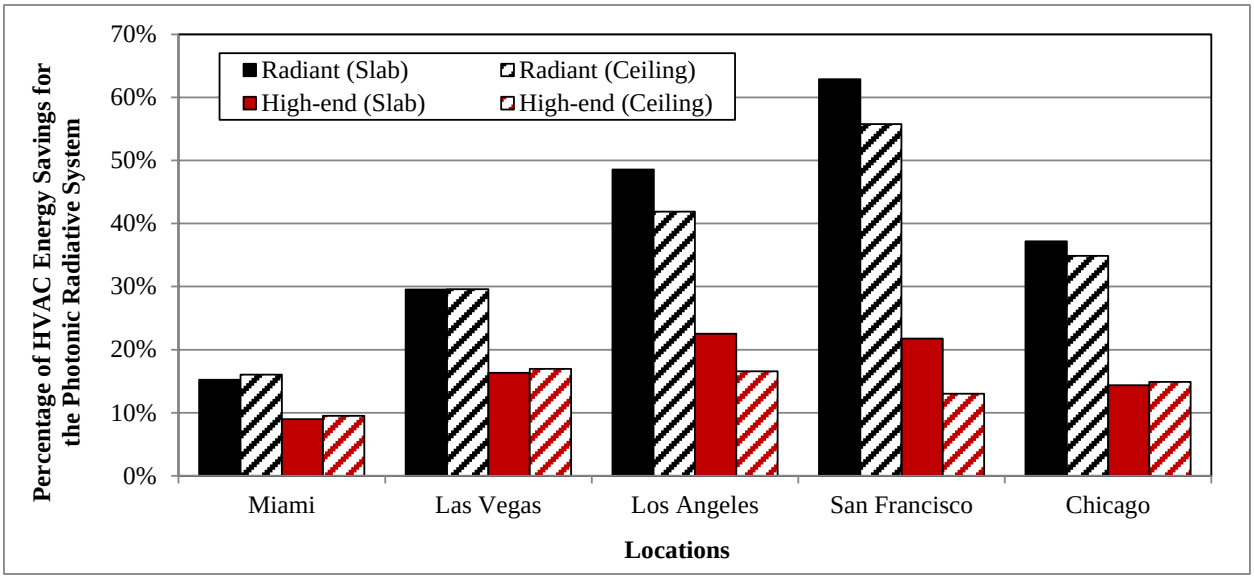

Figure 28: HVAC energy savings (percent) from the photonic system relative to the radiant system (Reference 2) and the high-end nighttime radiative cooling (Reference 3.2)

6. Market Analysis

A qualitative analysis is discussed in this section that identifies the technology components required to enable successful radiative cooling solutions in commercial buildings, the benefits of using radiative cooling, barriers to market adoption, and recommendations to overcome those barriers. The market analysis of radiative cooling is framed in the context of the prerequisite specification of radiant zone heating and cooling systems. Starting from the traditional approach of heating and cooling with VAV systems, photonic radiative cooling has to meet the following market decision thresholds:

- Do the benefits of adopting radiant cooling systems and the required suite of technology components (elaborated in Section 6.1) justify the additional costs and risks relative to conventional HVAC systems (VAV)?
- Do the additional benefits of adopting conventional radiative cooling and the additional required suite of technology components (elaborated in Section 6.2) justify the additional costs and risks associated with the additional radiative cooling components?

Do the benefits of adopting photonic radiative cooling (above and beyond conventional radiative cooling) justify the additional costs and risks associated with upgrades to photonic materials for the radiator?

6.1 Technology Components Required for Radiant Cooling

As described in the introduction, there are three general types of hydronic radiant cooling systems: radiant cooling panels, embedded surface systems, and thermally-active building systems. This section describes the various additional components of radiant cooling that are needed to create an integrated solution to heating and cooling a building, and why they all must be considered as required components.

- **Dedicated Outdoor Air Systems:** The provision of space cooling via radiant panels eliminates the general requirement of ducted air delivery in commercial buildings; however some form of provision of ventilation air is still required. This may take the form of a centralized DOAS with an efficient energy recovery ventilation component (e.g., enthalpy wheel). The much lower volumes of air required for ventilation (usually around 10% of the design air flow of a forced-air cooling system) mean that ductwork can be much smaller (e.g., small-diameter ductwork hung from the ceiling, as found in modern 'industrial' office space design) or that air delivery can utilize alternative pathways (exterior columns, small plenums) that avoid the need for ductwork above the ceiling and large inter-floor spaces. An alternative to a centralized DOAS is a building design that minimizes interior zones, allowing for zone-level DOAS at the envelope. This kind of system can eliminate ducts or other air pathways entirely, dramatically cutting fan energy requirements for the building.
- **Low-lift Variable-Speed Chillers:** . Because the hydronic loop is designed for high chilled water temperatures, and because the chiller is expected at most times only to supplement the radiative cooling (rather than provide the entire load), a chiller designed for high performance at part loads and with high chilled water temperatures is paramount. Previous energy modeling work (Katipamula et al. 2010) has shown that by using radiant cooling panels with thermal energy storage alone, 15% cooling savings can be achieved, but the savings jumps to over 45% with the addition of 'low-lift' vapor compression cooling equipment designed for part loads and warm chilled water temperatures.
- **Radiant Heating (Optional):** An optional component of the system, radiant heating is proposed as an additional system component because it can improve the total installed cost of the HVAC system by leveraging the same panels and tubing used for radiant cooling. In such a scenario, only a boiler, hot water pump, and minimum additional hot water piping would be required for heating the building. Switchover valves would be used zone-by-zone to control whether a zone receives heating or cooling. Depending on the building's configuration, solar heating load and

internal heat generation, radiant heating and cooling might need to be run simultaneously (in different zones) or, with more intelligent building design and zoning, seasonal or outdoor air temperature-based switchover points could be used to lock out the heating or cooling system entirely.

6.2 Technology Components Required for Radiative Cooling

This section describes the various additional components of radiative cooling above and beyond the components required for radiant systems. These additional components are needed to integrate the rooftop radiator into the radiant cooling system in a way that effectively makes use of the cooling available from the radiator.

- **Thermal Energy Storage:** the need for thermal energy storage arises as a consequence of the mismatch in timing of the environmentally-driven supply of radiant cooling and the demand for space cooling within most commercial buildings. This mismatch can potentially be mitigated somewhat by facilitating daytime radiative cooling, as claimed by the Stanford team (Raman et al. 2014) in regards to their photonic radiator. Regardless of the device, however, the integration of thermal energy storage into a holistic radiative cooling system design will greatly improve the performance of the system.

  Thermal energy storage can either be passive or active. Passive thermal storage involves embedding radiant tubing into high thermal-mass structures (e.g., concrete slabs between floors) or through interior structures filled with phase-change materials (with melting points close to room temperature) within the building, and running water in a loop through the radiator and slabs when outdoor conditions are favorable – generally at night. Active thermal energy storage involves using a large water tank as a storage medium for the radiative cooling generated at night, then using a separate water loop to draw cooled water from the tank and deliver it to radiant cooling panels throughout the building during times of space cooling demand.

- **Advanced Controls:** For simpler radiative cooling systems, advanced controls may not be necessary. Simple thermostatic controllers can be used to turn on and shut off the radiative cooling loop, and the supplemental chiller can run according to standard control settings in its dedicated control panel. As systems become more complex (for example, separate radiative and building cooling loops coupled by a thermal storage tank), advanced controls become increasingly necessary to achieve energy savings/prevent waste and to mitigate the potential for unmet heating and cooling loads. Three potentially valuable advanced control features include:

  - Chilled water temperature reset: Keeping in mind that the amount of free radiative cooling that can be emitted by the rooftop radiator increases as the water temperature delivered to the radiator increases, it is critical to supply the radiator with water that is as warm as possible, given the demands of the building for cooling. This means keeping the temperature of water supplied to radiant systems as warm as possible to keep the most demanding zone at or close to its cooling set point. The point of control is the discharge temperature for the supplemental chiller. A control algorithm that takes into account deviation of zone temperatures from their cooling set point is recommended to dynamically reset the chilled water temperature.

  - Radiant heating/cooling switchover: Systems that utilize both radiant heating and cooling with the same radiant panels will benefit greatly from advanced controls to judiciously switch from heating to cooling. Control algorithms are needed to maintain stable system operation without frequent heating/cooling switchovers and the compromise of thermal comfort.

- Peak shifting: Although not a control strategy needed to regulate the radiative cooling itself, a peak shifting algorithm can produce significant cost savings and some energy savings as well (using the chiller when it is more efficient to do so – e.g., at night) by intelligently using the chiller and thermal energy storage during hot weather. In peak summer cooling conditions, radiative cooling may not be available, but the chiller can be configured to run at night to store chilled water for use during daytime, flattening peak consumption.

6.3 Benefits

There are a wide variety of mechanisms by which radiant cooling and its required set of technologies can produce benefits to building owners and occupants. These include energy savings (and associated energy cost savings), other cost savings from elimination of alternative HVAC infrastructure and downsizing of equipment, plus a few side benefits. Table 6 details the mechanisms for energy and cost savings by the component technology of a holistic radiant cooling design. Likewise, Table 7 details the mechanisms for energy and cost savings for additional component technologies as part of radiative cooling systems.

Table 6: Summary of benefits from radiant cooling, by technology component

Technology	Energy Savings	Cost Savings and Side Benefits
Radiant Cooling Panels	Substantial electricity savings is realized relative to forced air cooling systems because of major downsizing or elimination of supply fans. Chiller energy savings is realized from the ability to use much warmer chilled water temperatures.	Radiant cooling panels carry their own significant installation costs; however, these costs are mitigated or overcome by the potential to eliminate ductwork, eliminate plenum spaces between floors (potentially shortening the building height), and significantly downsize or eliminate air-side fans, and associated instrumentation. Radiant cooling also leads to improved thermal comfort and indoor air quality.
Dedicated Outdoor Air System (DOAS) + Heat Recovery	Major energy savings in conditioning ventilation air is achieved through use of energy (heat and moisture) recovery with building exhaust air. Some minor energy savings is also achieved through separating sensible and latent cooling functions.	Energy cost savings accompany related energy savings. DOAS with heat recovery is very common in new buildings and recognized as a very cost-effective way to achieve energy savings. The system allows better humidity control, comfort and indoor air quality for building occupants.
Low-Lift Variable-Speed Chillers	Significant energy savings is achieved through better alignment of chiller peak performance with typical operating conditions (part load operation and high chilled water temperature).	Energy cost savings accompany related energy savings.
Radiant Heating	Radiant heating panels require dramatically lower hot water	Energy cost savings accompany related energy savings.

Technology	Energy Savings	Cost Savings and Side Benefits
	temperatures compared to forced air heating, meaning that if a condensing boiler is specified, thermal efficiencies can approach the boiler's maximum efficiency levels, which are typically above 97% (compared to between 70 and 80% for conventional boilers). With radiant heating, lower air temperatures are required to achieve the same degree of thermal comfort in heating mode, resulting in lower rates of heat loss through the envelope, and resulting energy savings.	Cost savings from elimination of ductwork and the leverage of existing infrastructure (radiant panels installed for cooling) for space heating.

Table 7: Summary of benefits from radiative cooling, by technology component

Technology	Energy Savings	Cost Savings and Side Benefits
Radiative Cooling Heat Exchangers	Rooftop heat exchangers will provide a significant fraction of annual cooling energy, offsetting electricity input to chillers.	The rooftop radiative cooling heat exchanger is expected to add a significant cost. This cost can be mitigated for new construction if the heat exchanger takes the place of an alternative exterior layer of roof construction. Electricity cost savings from free cooling will be realized every year the system runs.
Thermal energy storage (TES)	Thermal energy storage helps the chiller to realize significant savings from the use of radiative cooling by storing radiative cooling when it is available and using it when it is needed.	Facilitating load shifting from off peak to peak hours in places with large differences between daytime and nighttime rates can result in energy cost savings. This type of operation also opens the door to more advanced forms of demand response for grid services, if such programs become available.
Advanced Controls	Promotion of energy savings through optimization strategies and resets.	Elimination of potential scenarios that may lead to energy waste (cost increases) and discomfort for more complex systems.

6.4 Potential Barriers to Radiative Cooling Market Adoption and Recommendations

The following section details the barriers that likely exist to widespread market adoption and commercialization of radiative cooling.

6.4.1 Barrier 1: Poorly Suited for Retrofits

Discussion: The required use of radiant cooling panels make this technology generally infeasible for retrofits because radiant cooling panels involve casting/embedding chilled water tubing in building structural elements. In addition, the requirements for other major system components, such as dedicated outdoor air systems, may be incompatible with an existing building's ducting infrastructure and require major, expensive remodels. One of the most attractive pathways to market adoption is to take advantage of the initial design phase of building construction to intelligently specify radiant cooling systems in ways that eliminate the need for conventional technology approaches and save money on their elimination or downsizing. For retrofits, this advantage becomes a liability, in that legacy components have to be removed at extra cost, and no savings can be achieved through their avoidance.

Recommendations:

1a: **Target designers of new buildings** for adoption of this technology

OR

1b: Target building owners who are already planning a full building renovation (including envelope remodel). Every year, many existing building go through complete renovations that keep structural and load-bearing walls intact, but completely gut and rebuild the rest of the building. This may happen after major environmental damage to a building or for other reasons entirely. If an existing building is already slated to be 'gutted' and redesigned, this major construction project will not be accounted as a cost associated with the radiative system installation.

6.4.2 Barrier 2: Complexity and Holistic Design

Discussion: Unlike many technologies that can packaged and sold as a unit, radiative cooling is a solution to building cooling that requires the integration of several technologies, as detailed in this report. Building operations and maintenance (O&M) staff must understand how all parts of the system are designed to work together, what operating parameters to use, and how to troubleshoot problems. Currently, there is a lack of trained operators to manage the complex controls needed to run complex iterations of this system.

Recommendations:

2a: Market radiative cooling to building designers and architects as a defined solution set. If all of the identified components are sold, installed and commissioned by a single manufacturer, there is a greater likelihood of the components being sized correctly relative to one another, and being commissioned to run properly. By working with a single contractor, designers and architects will have a single point of contact to consult with regarding questions about the individual components, and they will come to understand how to integrate radiative cooling into the overall concept of the building from the earliest stages of design.

2b. Develop training programs to help O&M staff understand and manage the radiative cooling system and its components

OR

2c. Outsource O&M and troubleshooting of these systems to remote, third party contractors. An example of this type of model is the OptimumLoop (Optimum Energy 2015) all variable-speed chiller plant optimization service. A third party contractor installs variable-speed drives on all chiller

plant pumps and fans, plus a supervisory controller that they can remotely access and monitor to help client sites and troubleshoot problems.

6.4.3 Barrier 3: Installation Cost

Discussion: Several components are expected to carry significant first costs. These include the rooftop radiator, radiant cooling panels, thermal storage tank, and advanced controls infrastructure. Because of the need for large radiator surfaces, there is a need for cost containment in radiator design. Cost is a significant potential concern for the photonic radiator proposed by the Stanford team (Raman et al. 2014). Their radiator is similar in fabrication methods and complexity to solar photovoltaics panels. Solar photovoltaic (PV) may provide an expected order of magnitude approximation for installation costs on a dollar per square foot basis.

Recommendation:

3a. Offset installation costs with installation cost savings: As long as the focus is on new construction, there are several opportunities to save money on downsizing or eliminating alternative components. This cost savings should be subtracted from the sum of component-level installation costs in estimating the net installation cost (or savings):

- The rooftop radiator can serve as the exterior rooftop surface of the building, and replace the outermost layer of the built-up roof, saving on materials.
- Radiant cooling and heating panels can displace the need for large ductwork, and for inter-floor plenum spaces. There may be significant savings on building materials, ductwork and terminal box installation, etc. All air-handling units and/or rooftop units can be completely eliminated, and replaced with a single dedicated outdoor air system with a single pair of much smaller fans.
- If DOAS can be handled on the zone-level rather than using a centralized DOAS system, additional cost savings can be realized through elimination of all building ductwork.
- Substantial reductions in sizing of chillers and boilers may be possible, saving cost through specification of smaller units.

3b. Develop PV/T products with the capability of radiative cooling. In recent years, much work was done to combine PV modules for electricity generation and solar collectors for heating generation resulting in hybrid PV/T (PV and thermal) collectors, which can be installed as an essential component of the building envelope (typically a roof). Currently, night radiators and PV/T collectors are separate devices and used for different purposes; radiators operate at night for cooling while PV/T collectors operate during the day for heating and electricity generation. Operating PV/T collectors for cooling utilize one single device for multiple uses, which can potentially increase the return rate on investment.

3c. In U.S. regions with water shortages, use combined radiative/evaporative cooling rooftop heat exchangers. While it is understood that Department of Energy (DOE) does not want to solve energy problems by creating water problems, water supply concerns are regional in nature, and certain regions with ample water and expensive energy may benefit from approaches that use evaporative cooling to boost energy savings and lower installed cost. The idea is that letting water run freely over the surface of the roof will be a much lower cost solution than maintaining a closed water loop and coupling that to a large-area heat exchanger. For example, the WhiteCap roof spraying system (Collins and Parker 1998) was reported to have an installation cost for the rooftop spray system of \$400 per 1000 ft^2 of roof surface (in 1998 dollars). Even in today's dollars, this is likely to be much less expensive than closed-loop, custom rooftop radiator installations.

3d. Verify that expected energy cost savings of the Stanford photonic radiator justifies expected additional installation cost above and beyond conventional approaches to radiator design. Pacific

Northwest National Laboratory (PNNL) will address the savings question with modeling work. The cost of the photonic products at production scale are not known at this time. So, DOE can evaluate favorability based on its own metrics for payback/amortization of initial costs.

3e. Evaluate and focus on market segments where technology has the highest value proposition. For example, government and other institutional facilities that are more accepting of technologies with longer paybacks could act as a catalyst for this technology.

6.4.4 Barrier 4: Limitations on Building Suitability by Shape

Discussion: Radiative cooling to satisfy a substantial fraction of building cooling loads, requires a relatively large ratio of rooftop radiator area to building floor area. For this reason, this technology may not be suited for tall buildings (more than three stories).

Recommendations:

4a. Target installation on shorter buildings. Almost 90% of buildings are small- and medium-sized, accounting for about almost half the energy consumption and conditioned area. These buildings should be the targets for the proposed technology.

4b. Make any interested building designers aware of this limitation. Educating the building designers and owners of the benefit of radiative cooling could lead to buildings with sufficient roof area (or fewer stories).

6.4.5 Barrier 5: Space Concerns

Discussion: Many small- and medium-sized commercial buildings are not designed with large mechanical spaces to house a chiller and a large thermal energy storage tank (the expected size is 10,000 gallons for a 50,000 square foot building based on our current modeling work).

Recommendation:

5a. Install large equipment on outdoor pad. If a large mechanical space cannot be worked into the building design, some mechanical equipment can be placed on a pad outdoors. The storage tank should be situated in a shaded location and well insulated if it is placed outside.

6.4.6 Barrier 6: Familiarity and Customer Acceptance Level

Discussion:

- Radiative cooling heat exchangers are a very rare and unfamiliar technology. Radiative cooling systems were installed by a few very small companies in some niche markets, especially in the 1990s, but have not seen major market acceptance or penetration. Unfamiliarity with this technology may lead to risk-aversion, or may simply keep this technology "off the radar."
- Customer acceptance is poor in some cases for radiant cooling panels because of perceptions about condensation problems. Like many emerging technologies (heat pumps in 1970s, thermal storage systems in 1980s), some early problems with the rollout of this technology contribute to this perception.
- For low-lift variable-speed chillers, there is limited familiarity among operators and contractors because few major HVAC suppliers provide variable-speed compressors and their product range is limited.
- Building operators may also have aversion to the use of advanced controls

Recommendations:

6a. Fund and highlight technology demonstration sites and address customer concerns. Be sure that in humid climates, radiant panels are paired with DOAS systems with low supply air temperature set

points (below 53°F) that will effectively limit indoor humidity levels and prevent condensation. Indoor humidity sensors should be used to prevent chilled water supply temperatures from going below the indoor dewpoint temperature. Develop and publish informational resources with lessons learned from local case studies to increase understanding of the technology.

6b. Scale and commercialize radiative cooling products. Currently, there are not many commercial radiative cooling products that can be readily installed for building space cooling. In particular, the innovative daytime radiant cooling technology developed by Stanford is still at the laboratory prototype stage, although a lot of work is underway to develop technologies for scaling photonic radiative cooling surfaces.

6c. Clearly identify the niche of market that is suitable for the application of radiative cooling technologies. The current work being done by PNNL will provide insights on the impact of different climate on the savings potential of radiative cooling technologies. More work needs to be done regarding the impact of different building types.

6.4.7 Barrier 7: Climate Constraints

Discussion: Locations with the following summer climate characteristics may limit the impact of radiative cooling.

- Climates where the majority of summer nighttime hours are very warm (over 80°F),
- Climates where the majority of nighttime hours are warm and humid (over 80% relative humidity, with temperatures over 75°F)
- Climates with frequent hot summer days will limit the additional effectiveness of Stanford's photonic radiator.
- Far northern climates with very short summer nights
- Small buildings in marine climates with low to zero cooling demands.

Recommendation:

7a.Target favorable climates for technology demonstration and marketing (warm days, cool nights, low humidity). PNNL will address the level of expected savings by climate location with the current modeling work.

7. Conclusions

Recent advances in materials have demonstrated the ability to maintain radiator surfaces at below-ambient temperatures in the presence of intense, direct sunlight. These materials have spectrally selective properties: high reflectance for the shorter wavelength range of the incoming solar radiation but low reflectance for the wavelength range where the atmosphere is transparent for thermal radiation. For the first time, an HVAC system integrating the use of the photonic radiative cooler was proposed and modeled using the whole energy simulation program EnergyPlus. A water storage tank and an air-cooled chiller were serially connected and sequentially controlled to provide cold water to a radiant slab hydronic zone distribution system.

Based on the simulation results for a 5,000-m^2 office building, the photonic radiator occupying about 60% (i.e., 984 m^2) of the roof area was sufficient to meet the cooling load in January, February, March, November, and December for locations not in very hot climates. For the cooling season (June to September), the free energy from the radiator addressed about 10% of cooling load in Miami, between 17% and 36% in Las Vegas, between 61% and 84% in Los Angeles, more than 90% in San Francisco, and between 26% and 63% in Chicago. The photonic radiative cooler provided significantly more free energy at daytime than the conventional nighttime radiative cooler, which demonstrates the desired daytime cooling potential from the novel technology. The difference was particularly evident in Miami, Las Vegas, and Los Angeles. For the photonic cooler, daytime charging contributed between 30% and 51% of the annual free cooling energy charged to the tank.

Relative to the best cool roof surfaces on the market that could conceivably be used as a competing radiator surface for nighttime radiative cooling, the photonic radiative cooler saved 10 MWh electricity in Miami, 13 MWh in Las Vegas, 8 MWh in Los Angeles, 3 MWh in San Francisco and 6 MWh in Chicago, per year, which represents 9%, 16%, 23%, 22%, and 14% of cooling electricity savings, respectively in the above five cities. To achieve a 5-year simple payback period, the maximum acceptable incremental cost for upgrading from nighttime cooling to photonic radiative cooling should range from $2.50 to $6.25 per square meter of the radiative cooling heat exchanger's surface area. To account for locations where high-end nighttime radiative cooling may not be economical in the first place, an accompanying economic analysis of the overall upgrade from VAV systems to photonic radiative cooling was performed. This analysis reveals that the incremental cost of all components of the combined radiative/radiant cooling system should not exceed $8.25 to $11.50 per square meter of total building floor area.

Several key component parameters such as storage tank size and radiative cooler area are expected to have a large impact on the system performance and incremental cost. Additional sensitivity analyses will be valuable to understand how the component sizing affects the results. It will be also worthwhile to expand the simulation analysis to more locations with different climates and more building types. Moreover, the system modeled in this work is only one possible design using photonic radiative coolers. It is by no means the best design or the most recommended system configuration. In this respect, many alternative systems could be evaluated and compared to explore their advantages and disadvantages. For example, the embedded surface radiant zone cooling system might be replaced with a thermally active building system, which may eliminate the use of a water storage tank utilizing building thermal mass instead. Another example is using the photonic radiator as a "dry" cooler in the condenser loop of a water-cooled chiller plant as a competing alternative to a cooling tower. This would have the potential to eliminate water losses that occur in cooling towers through evaporation by design. Closed water loops would also alleviate other concerns around maintenance of cooling towers (scale and algae accumulation for example) as well as health concerns that have recently surfaced around contraction of Legionnaires' Disease from Legionella bacteria growing in cooling towers. Finally, a more complete economic analysis using expected cost data may be beneficial to reveal how cost-competitive photonic radiative cooling, as envisioned in this report, is expected to be relative to the various alternatives.

References

Al-Obaidi KM, M Ismail and AMA Rahman. 2014. Passive cooling techniques through reflective and radiaitive roofs in tropical houses in Southeast Asia: A Literature Review. Frontiers of Architectural Research 3(3):283-297.

Alvine KJ, BE Bernacki, WD Bennett, DJ Edwards, and A Mendoza. 2013. Optical response of oriented and highly anisotropic subwavelength metallic nanostructure arrays. Applied. Physics Letters (102):201115.

Armstrong P, W Jiang, DW Winiarski, S Katipamula, and LK Norford. 2009. Efficient low-lift cooling with radiant distribution, thermal storage and variable-speed chiller controls Part II: Annual energy use and savings. HVAC&R Research 15(2):402-432.

ASHRAE. 2012. Handbook of HVAC Systems and Equipment. American Society of Heating, Refrigerating and Air Conditioning Engineers, Inc., Atlanta, GA.

ASHRAE. 2013. ANSI/ASHRAE Standard 55-2013: Thermal Environmental Conditions for Human Occupancy. American Society of Heating, Refrigerating and Air Conditioning Engineers, Inc., Atlanta, GA.

Aubinet M, 1994. Longwave sky radiation parametrizations. Solar Energy 53(2):147–154.

Babiak J, BW Olesen, and D Petras. 2009. Low Temperature Heating and High Temperature Cooling. Federation of European Heating and Air-Conditioning Associations, Brussels, Belgium.

Berdahl P. 1984. Radiative cooling with MgO and/or LiF layers. Applied Optics 23(3):370-372.

Bourne R and MA Hoeschele. 2000. Applying natural cooling to slab floors. In Proceedings of ACEEE Summer Study on Energy Efficiency in Buildings. Washington, DC. American Council for an Energy-Efficient Economy, Washington, D.C. Accessed October 23, 2015 from http://www.aceee.org/files/proceedings/2000/data/papers/SS00_Panel3_Paper03.pdf

Budd D and JW Lang. 2014. Sustaining by reserving. High Performance Building, Spring Issue, 62-70.

Carpenter SC and JP Kokko. 1998. Radiant heating and cooling, displacement ventilation with heat recovery and storm water cooling: an environmentally responsible HVAC system. ASHRAE Transactions 104(2):1321-1326.

Catalanotti S. 1975. The radiative cooling of selective surface. Solar Energy (17):173-178.

Cavelius R, C Isaksson, E Perednis, and G Read. 2007. Passive Cooling Technologies: Evaporative Cooling, Radiative Cooling, Night Ventilation, Earth to Air Heat Exchangers, Energy Ponds, Groundwater/Sea/River/Lake Water Cooling, Cooling Towers. Austrian Energy Agency. Vienna, Austria.

Clark G and C Allen. 1978. The estimation of atmospheric radiation for clear and cloudy skies. In Proceedings 2nd National Passive Solar Conference (AS/ISES). pp. 675-678. Mid-Atlanta Solar Energy Association, Philadelphia, PA.

Clear RD, L Gartland and FC Winkelmann. 2001. An Empirical Correlation for the Outside Convective Air Film Coefficient for Horizontal Roofs. Lawrence Berkeley National Laboratory. Report # LBNL-47275. Berkeley, CA.

Collins T and S Parker. 1998. Technology Installation Review: WhiteCap Roof Spray Cooling System. Pacific Northwest National Laboratory, Richland, WA. Accessed October 23, 2015 from http://www.builditsolar.com/Projects/Cooling/WhitecapRoofCoolingReport.pdf

Corbin CD, GP Henze, and P May-Ostendorp. 2013. A model predictive control optimization environment for real-time commercial building application. Journal of Building Performance Simulation (6):159-174.

CRRC. 2015. Cooling Roof Rating Council: Rated products directory. URL: http://coolroofs.org/products, last accessed in May 2015.

Doebber I, M Moore, and M Deru. 2010. Radiant slab cooling for retail. ASHRAE Journal, December Issue, 28-38.

EIA (Energy Information Administration). 2015. Electricity and Natural Gas Prices. Retrieved in July 2015 from http://www.eia.gov/electricity/data.cfm#sales and http://www.eia.gov/dnav/ng/ng_pri_sum_dcu_nus_m.htm.

Eicker U and A Dalibard. 2011. Photovoltaic-thermal collectors for night radiative cooling of buildings. Solar Energy (85):1322-1335.

Epstein RI, MI Buchwald, BC Edwards, TR Gosnell and CE Mungan. 1995. Observation of laser-induced fluorescent cooling of a solid. Nature (377):500-503.

Eriksson TS and CG Granqvist. 1986. Infrared properties of Silicaon Oxynitride Filens: experimental data and theoretical interpretation. Journal of Applied Physics (60):2081.

Feng J. 2014. Design and Control of Hydronic Radiant Cooling Systems. Ph.D. Thesis. University of California, Berkeley.

Feng J, S Scjoavon, and F Bauman. 2013. Cooling load differences between radiant and air systems. Energy and Buildings (65): 310-321.

Feng J, F Chuang, F Borrelli, and F Bauman. 2015. Model predictive control of radiant slab systems with evaporative cooling sources. Energy and Buildings (87):199-210.

Feustel HE and C Stetiu. 1995. Hydronic radiant cooling – preliminary assessment. Energy and Buildings (22): 193-205.

Gentle AR and GB Smith. 2010. Radiative heat pumping from the earth using surface phonon resonant nanoparticles. Nano Letters (10):373-379.

Granqvist CG and A Hjortsberg. 1981. Radiative cooling to low temperatures: general considerations and application to selectively emitting SiO films. Journal of Applied Physics (52):4205.

Granqvist CG. 2003. Solar energy materials. Advanced Materials 15(21):1789-1803.

Hamilton SD, KW Roth, and J Brodrick. 2004. Displacement ventilation. ASHRAE Journal, September Issue, 56-58.

Hastbacka M, J Dieckmann, and A Bouza. 2012. DOAS and radiant cooling revisited. ASHRAE Journal, December Issue, 128-130.

Henze GP, C Felsmann, DE Kalz, S Herkel. 2008. Primary energy and comfort performance of ventilation assisted thermos-active building systems in continental climates. Energy and Buildings 40 (2): 99-111.

Houghton D. 2006. Radiant night-sky heat rejection and radiant cooling distribution for a small commercial building. American Council for an Energy Efficient Economy (ACEEE), Washington, D.C. In Proceedings of ACEEE Summer Study on Energy Efficiency in Buildings. Pacific Grove, CA. Accessed November 2015 from http://aceee.org/files/proceedings/2006/data/papers/SS06_Panel3_Paper12.pdf

Hu R and JL Niu. 2012. A review of the application of radiant cooling and heating systems in Mainland China. Energy and Buildings (52):11-19.

Incropera FP, DP DeWitt, TL Bergman and AS Lavine. 2007. Fundamentals of Heat and Mass Transfer-6th Edition. Empirical Correlations: External Free Convection Flows. p. 571-577. John Wiley and Sons. Hoboken, NJ.

ISO. 2012. ISO 11855. Building environment design - Design, dimensioning, installation and control of embedded radiant heating and cooling systems - Part 2: Determination of the design heating and cooling capacity. International Organization for Standardization. Geneva, Switzerland.

Jeong J, SA Mumma, and WP Bahnfleth. 2003. Energy conservation benefits of a dedicated outdoor air system with parallel sensible cooling by ceiling radiant panels. ASHRAE Transactions 109(2):627-636.

Katipamula S, Armstrong PR, Wang W, Fernandez N, Cho H, Goezler W, Burgos, J, Radhakrishana R, Ahlfeldt C. 2010. Develmopment of a High-Efficiency Low-Lift Vapor Compression System – Final Report. Pacific Northwest National Laboratory. PNNL-19227. Richland, WA.

Krajcik M, R Tomasi, A Simone, and B Olesen. 2013. Experimental study including subjective evaluations of mixing and displacement ventilation combined with radiant floor heating/cooling system. HVAC&R Research (19):1063-1072.

Mastai Y, Y Diamant, T Aruna and A Zaban. 2001. TiO2 Nanocrystalline pigmented polyethylene foils for radiative cooling applications: Synthesis and Characterization Langmuir (17):7118-7123.

Mihalakakou G, A Ferrante, and JO Lewis. 1998. The cooling potential of a metallic nocturnal radiator. Energy and Buildings (28):251-256.

Meir MG, JB Rekstad and M Lovvik. 2002. A study of a polymer-based radiative cooling system. Solar Energy 73(6):403-417.

Memon RA, S Chirarattananon, and P Vangtook. 2008. Thermal comfort assessment and application of radiant cooling: A case study. Building and Environment (43):1185-1196.

Mumma S. 2002. Chilled ceilings in parallel with dedicated outdoor air systems: addressing the concerns of condensation, capacity, and cost. ASHRAE Transactions 108 (2):220-231.

Nall D. 2013a. Thermally active floors, Part 1. ASHRAE Journal, January Issue, 32-46.

Nall D. 2013b. Thermally active floors, Part 2. ASHRAE Journal, February Issue, 36-46.

Nall D. 2013c. Thermally active floors, Part 3. ASHRAE Journal, March Issue, 54-61.

Niklasson GA and TMJ Nilsson. 1995. Radiative cooling during the day: simulations and experiments on pigmented polyethylene cover foils. Solar Energy Materials and Solar Cells 37(1): 93-118.

Nilsson TMJ, GA Niklasson and CG Granqvist. 1992. A solar reflecting material for radiative cooling applications: ZnS Pigmented Polyethylene. Solar Energy Materials and Solar Cells (28):175.

Niu JL, LZ Zhang, and HG Zuo. 2002. Energy savings potential of chilled-ceiling combined with desiccant cooling in hot and humid climates. Energy and Buildings (34):487-495.

Novoselac A and J Srebric. 2002. A critical review on the performance and design of combined cooled ceiling and displacement ventilation system. Energy and Buildings (34):497-509.

Nutprasert N and P Chaiwiwatworakul. 2014. Radiant cooling with dehumidified air ventilation for thermal comfort in buildings in tropical climate. Energy Procedia, (52):250-259.

Oak Ridge National Laboratory. 2014. “Night Sky” System Cools Roof Tops, Saves Energy. Oak Ridge TN Accessed December 15, 2014 from http://web.ornl.gov/sci/eere/international/Website/Nightsky%20Cools%20RoofTops.htm.

Olesen B. 2008. Radiant floor cooling systems. ASHRAE Journal, September Issue, 16-22.

Olesen B. 2012. Thermo active building systems: Using building mass to heat and cool. ASHRAE Journal, February Issue, 44-52.

Optimum Energy. 2015. OptimumLOOP. Accessed June 11, 2015 from http://optimumenergyco.com/wp-content/uploads/2014/07/OptimumLOOP-Overview-7.30.2014.pdf

Parker, D. 2005. Theoretical Evaluation of the NightCool Nocturnal Radiation Cooling Concept. Prepared by the Florida Solar Energy Center, Cocoa, FL for the U.S. Department of Energy, Washington, D.C. FSEC-CR-1502-05..

Raeissi S and M Taheri. 2000. Skytherm: an approach to year-round thermal energy sufficient houses. Renewable Energy 19(4):527-543.

Raman AP, MA Anoma, L Zhu, E Raphaeli and S Fan. 2014. Passive radiative cooling below ambient air temperature under direct sunlight. Nature (515):540-544.

Rephaeli E, A Raman and S Fan. 2013. Ultraband photonic structures to achieve high-performance daytime radiative cooling. Nano Letters 13(4):1457-1461.

Sastry G and P Rumsey. 2014. VAV vs. Radiant side-by-side comparison. ASHRAE Journal, May Issue, 16-24.

Shen L, F Xiao, H Chen, and S Wang. 2013. Investigation of a novel thermoelectric radiant air-conditioning system. Energy and Buildings (59):123-132.

Simmonds P, S Holst, S Reuss, and W Gaw. 2003. Using radiant cooled floors to condition large spaces and maintain comfort conditions. ASHRAE Transactions 106 (1):695–701.

Stetiu C. 1999. Energy and peak power savings potential of radiant cooling systems in US commercial buildings. Energy and Buildings (30):127-138.

Strand RK and CO Pedersen. 2002. Modeling radiant systems in an integrated heat balance based energy simulation program. ASHRAE Transactions 108(2):1-9.

Talbot M. 2013. Collaborative. High Performance Building. Summer Issue, 6-17.

Tazawa M, H Kakiuchida, G Xu, P Jin and H Arwin. 2006. Optical constants of vacuum evaporated SiO film and an application. Journal of Electroceramics 16(4):511-515.

Tian Z and JA Love. 2009a. Energy performance optimization of radiant slab cooling using building simulation and field measurements. Energy and Buildings (41):320-330.

Tian Z and JA Love. 2009b. Application of radiant cooling in different climates: assessment of office buildings through simulation. In Proceedings of 11th International IBPSA Conference, Glasgow, UK, pages 2220-2227. International Building Performance Simulation Association.

Timothy M, B Fred, and H Charlie. 2006. Radiant cooling research scoping study. Center for the Built Environment, University of California, Berkeley CA. Accessed October 23, 2015 from http://www.cbe.berkeley.edu/research/pdf_files/IR_RadCoolScoping_2006.pdf

Thornton BA, W Wang, MD Lane, MI Rosenberg, and B Liu. 2009. Technical Support Document: 50% Energy Savings Design Technology Packages for Medium Office Buildings. PNNL-18774, Pacific Northwest National Laboratory, Richland, WA.

Thornton BA, MI Rosenberg, EE Richman, W Wang, YL Xie, J Zhang, H Cho, VV Mendon, RA Athalye, and B Liu. 2011. Achieving the 30% Goal: Energy and Cost Savings Analysis of ASHRAE Standard 90.1-2010. PNNL-20405, Pacific Northwest National Laboratory, Richland, WA.

U.S. Department of Energy (DOE). 2013. EnergyPlus Engineering Reference – The Reference to EnergyPlus Calculations. Washington, D.C. Updated October 1, 2013.

U.S. Department of Energy (DOE). 2015. Commercial Prototype Building Models, Building Energy Codes Program, Department of Energy. Accessed January 2015 from https://www.energycodes.gov/commercial-prototype-building-models

Vangtook P and S Chirarattananon. 2007. Application of radiant cooling as a passive cooling option in hot humid climate. Building and Environment (42):543-556.

Weitzmann P, E Pittarello, and BW Olesen. 2008. The cooling capacity of the thermo active building system combined with acoustic ceiling. In Proceedings of the 8th Symposium on Building Physics in the Nordic Countries, Copenhagen, Denmark. Danish Society of Engineers, IDA. Accessed October 23, 2015 from http://web.byv.kth.se/bphys/copenhagen/pdf/269-2.pdf

Zakula T, PR Armstrong, and L Norford. 2015. Advanced cooling technology with thermally activated buildingsurfaces and model predictive control. Energy and Buildings (86):640-650.

Zhang S and J Niu. 2012. Cooling Performance of Nocturnal Radiative Cooling Combined with Microencapsulated Phase Change Material (MPCM) Slurry Storage. Energy and Buildings (54):122-130.

Zhang T, X Liu, L Zhang, J Jiang, M Zhou, and Y Jiang. 2013. Performance analysis of the air-conditioning system in Xi'an Xianyang International Airport. Energy and Building (59):11-20.

Zhu L, A Raman and S Fan. 2013. Color-preserving daytime radiative cooling. Applied Physics Letters 103.

Zhu L, A Raman, KX Wang, MA Anoma, and S Fan. 2014. Radiative cooling of solar cells. Optica 1(1): 32-38.